The role of Wnt5 during Axon guidance

Wouda, R.R.

Chapter 6

Antagonistic Roles of Wnt5 and the Drl RYK Receptor in Patterning The *Drosophila* Antennal Lobe

*Nature Neuroscien*ce **10**, 1423 - 1432 (2007)

Antagonistic Roles of Wnt5 and the Drl RYK Receptor in Patterning the Drosophila Antennal Lobe

Yuping Wu[1] *, Ying Yao[2]*, Chong Yin[1]*, Rie Ozawa[2], Toshiro Aigaki[3], Rene R. Wouda[4], Jasprina N. Noordermeer[4], Lee G. Fradkin[4] and Huey Hing[1, 2]

Cell and Developmental Biology[1], Neuroscience Program[2], University of Illinois at Urbana-Champaign 601 South Goodwin Avenue Urbana, Illinois 61801

Biological Sciences[3], Tokyo Metropolitan University 1-1 Minami-osawa, Hachioji-shi Tokyo 192-0397, Japan

Laboratory of Developmental Neurobiology[4], Department of Molecular Cell Biology Leiden University Medical Center Einthovenweg 20 2300 RC Leiden, The Netherlands

Abstract

Numerous studies showed that ingrowing olfactory axons exert inductive influences on olfactory map development. From an overexpression screen, we identified wnt5 as a potent organizer of the olfactory map in Drosophila. Loss of wnt5 results in severe derangement of the glomerular pattern, while overexpression of wnt5 results in the formation of ectopic midline glomeruli. Cell-type specific cDNA rescue and mosaic experiments show that wnt5 functions in the olfactory neurons. Mutation in the derailed (drl) RYK gene, encoding a receptor for Wnt5 results in derangement of the glomerular map, ectopic midline glomerular development and the accumulation of Wnt5 at the midline. We show that drl functions in glial cells, where it acts upstream of wnt5 to modulate its function in glomerular patterning. Our findings establish wnt5 as an anterograde signal expressed by olfactory axons and demonstrate a previously unappreciated, yet powerful, role for glia in patterning the Drosophila olfactory map.

Key Words: Wnt, Drl, Ryk, Olfactory, Glomerulus, Dendrites, Synaptogenesis

* These authors contribute equally to this work

Introduction

The perception of odors requires that stimulus information be systematically organized in a "map" in the olfactory bulb. Indeed, axons of olfactory receptor neurons (ORNs) expressing a given odorant receptor (OR) sort out from other axons and terminate specifically within one of a field of discrete synaptic structures, termed glomeruli, in the olfactory bulb[1]. Previous studies showed that the pattern of glomeruli, or olfactory map, is a direct result of precise axon pathfinding and synaptogenesis[2,3]. Recent work in several species has identified a number of molecules that are necessary for the proper development of the olfactory map. These molecules include transmembrane proteins such as Ncam-180, Neuropilin-1, Robo, the odorant receptors, Dscam, and Cadherin, as well as cytoplasmic signalling molecules such as Src, Fyn, Dock and Pak4-9. An attempt to integrate these diverse mechanisms has led to the hierarchical model of ORN axon targeting, wherein ORN axons are sequentially guided towards their postsynaptic

targets with increasing degree of precision[4,5]. A wealth of evidence shows that ingrowing ORN axons play a pivotal role in directing the development of the glomeruli in *Drosophila* and other species. First, genetic or surgical disruption of the ORN axons blocks the formation of the glomeruli, indicating that ORN axons are necessary for glomerular development[10,11,6]. Second, when the Lim Kinase gene is overexpressed in the ORNs, or when the ORNs are transplanted to ectopic sites, the axons direct the formation of glomeruli in ectopic positions, indicating that the presence of ORN axons is also sufficient for glomerular development[12,10,13,14]. It has been suggested that ORN axons have an intrinsic ability to specify glomerular development in their target tissues[15], but the underlying mechanisms are unknown.

The *Drosophila* olfactory system is highly suited for unraveling the mechanisms of olfactory map development. The anatomy and development of the fly antennal lobe (AL) bears close resemblance to the olfactory bulb of mammals but is vastly simpler, containing only 43 glomeruli compared with ~2,000 in the mouse. Fly ORNs are located in the antennae and the maxillary palps. From these appendages, ORN axons project to the AL, where they synapse with the dendrites of the projection neurons (PNs) in specific glomeruli[16], which in turn feed into the higher brain centers. As in vertebrates, neurons expressing a given OR gene extend axons that converge on a spatially invariant glomerulus in the AL[17,18]. The anatomic simplicity of the fly AL, combined with the ability to manipulate single molecules and specific cell types in vivo, make Drosophila an ideal system to probe the molecular mechanisms of odor map formation.

To dissect the mechanisms of odor map development, we have conducted an overexpression screen for genes that disrupt the stereotyped anatomy of the Drosophila AL. We identified *wnt5* as a candidate regulator of AL development. The *wnt5* gene encodes a member of the large evolutionarily-conserved Wnt family of secreted proteins which have well-established roles in embryonic patterning, cell proliferation and cell differentiation[19,20]. Recent studies show that Wnt5 functions as a repulsive cue that route axons through the correct commissures of the embryonic ventral midline[21] and regulate their fasciculation[22], and is required for stabilizing a subset of axons in the adult brain[23]. We show here that *wnt5* functions in the ORNs to regulate the patterning of the olfactory glomeruli. In the absence of *wnt5*, ORN axons mistarget, and the glomerular map is disorganized. We also provide evidence that the Derailed (Drl) Ryk family receptor tyrosine kinase, previously demonstrated to act as a repulsive neuronal Wnt5 receptor in the embryonic CNS21, functions in glia to inhibit Wnt5 signalling. Our molecular dissections of the Drl protein suggest that it inhibits Wnt5 through its extracellular WIF (Wnt inhibitory factor) domain. Our results demonstrate that Wnt5 is an anterograde signal by which ORN axons specify the organization of the olfactory, map and that Drl, presented by glial cells, is a powerful modulator of this signal.

Methods

Experimental Animals

The *P{GS} Drosophila* lines were generated by *Drosophila* Gene Search Project, Tokyo, Metropolitan University[45]. The *Or-Gal4* and *Or-MCD8-GFP (Or-mGFP)* lines were from L. Vosshall and B. Dickson, and the *UAS-drl*$^{\Delta cyto}$ line was from J. Dura[39], and the *72OK-Gal4* line was kindly provided by K. Ito. The construction of the *GH-mGFP* line has been described[14]. Other stocks, referenced throughout the text, were obtained from Bloomington *Drosophila* Stock Center.

Transgenes

Full-length *drl* cDNA (from Open Biosystems) was subcloned into *pUAST* vector to generate *UAS-drl*. To create *UAS-drl*^{K371A}, a fragment of the *drl* coding region (bps 1079-1830) bearing the K371A mutation was generated by PCR, fused in frame with the remainder of the *drl* coding region and then cloned into *pUAST*. To generate *UAS-drl*$^{\Delta WIF}$, a DNA fragment from nucleotide 472 to 1830, which lacks the WIF-encoding sequences, was generated by PCR, fused with the first 60 nucleotides of *drl* coding region, and then subcloned into *pUAST*. Transgenic animals were generated by standard procedures.

Immunohistochemistry

Adult (1 to 2 days old) or pupal brains were quickly dissected in cold phosphate buffered saline (PBS, 130 mM NaCl, 10 mM Na_2HPO_4, pH 7.2) and fixed in PLP (2% paraformaldehyde, 0.25% sodium periodate, 75 mM lysine-HCl and 37 mM sodium phosphate pH 7.4) for 1 hour. The fixed brains were wash with PBST (PBS with 0.5% Triton-X-100) and stained with the primary antibodies overnight. For Wnt5 staining, dissected brains were directly stained with anti-Wnt5 antibody in PBS (2.5 hours at 4°C), wash with PBS with goat serum, followed by fixation in PLP (1 hour, 25°C). Subsequent steps are the same as below. mAb nc82 (1:20) was gift from A. Hofbauer[26]; rabbit anti-GFP (1:100) was obtained from Molecular Probes; rat anti-mCD8 mAb (1:100) was from Caltag. Affinity purified rabbit anti-Wnt5[22] and rabbit anti-Drl were both used at 1:100 dilutions. The anti-Drl antiserum was raised against a GST fusion protein including Drl amino acids 123-222 and was affinity purified against the same protein coupled to a column. The secondary antibodies, FITC-conjugated goat anti-rabbit, Cy3-conjugated goat anti-mouse and FITC-conjugated goat anti-rat, were obtained from Jackson Laboratories and used at 1:100 dilution.

Results

wnt5 Overexpression in the ORNs Disrupts Antennal Lobe Structure

From a screen of 3,996 *P{GS} Drosophila* lines[24], we found that the overexpression of *wnt5* (*P{GS1}1192*), under the control of the *SG18.1-Gal4* driver, which is preferentially expressed in the ORNs[25,6], profoundly altered the anatomy of the AL. To assess the effect of *wnt5* overexpression, we labeled different ORN subsets with GFP and also stained the ALs with the nc82 mAb[26], which stains the presynaptic Bruchpilot protein[27], highlighting the individual glomeruli. In the wild-type adult expressing GFP under the control of *SG18.1-Gal4*, the ALs are spherical (~70 μm diameters), contain distinct glomeruli, and are connected by a commissure ~20 μm thick (**Fig. 1a**). In the *wnt5* overexpressing animals, the ALs were malformed and had irregularly shaped glomeruli (**Fig. 1b**). Glomerulus-like structures appear in the commissure in 79% of the ALs, significantly enlarging the structure to ~60 μm in thickness (**Figs. 1a, b**). To examine the arrangement of the glomeruli, we labeled a lateral glomerulus (*Or47b*, **Figs. 1c, d**) and two medial glomeruli (*Or22a*, *Or43b*, **Figs. 1e, f, j, k**). We observed that a large percentage of the glomeruli in the *wnt5*-overexpressing animals are split into multiple subunits, many of which are displaced dorsally, including to the midline region (arrowheads, **Figs. 1d, f**). Examination of the *Or43b* glomerulus, reveals that it is dorsally displaced in 93% (13/14) of the brains (**Fig. 1j, k**). The termination of ORN axons in ectopic positions indicates that ORN axons were misguided in the *wnt5*-overexpressing animals. On the average, 77.1% of the *wnt5*-

overexpressing brains showed ectopic projections of ORN axons and 51.9% of the brains showed ectopic glomeruli at the midline (**Fig. 1k**).

To assess the morphology of the PNs, we used the *GH-mGFP* transgene, which labels a subset of these cells revealing their dendritic arbors[14]. In the wild type, PNs extend their dendrites into the AL, where they innervate specific glomeruli, creating a pattern of dendritic arbors (**Fig. 1g**). In the *P{GS1}1192; SG18.1-Gal4* animal, the organization of the dendritic arbors appeared disrupted, a subset even invaded the midline, where they innervate the ectopic glomeruli (asterisk, **Fig. 1h**). The structure of the *wnt5* gene, the positions of the *P{GS}* insertions and the extent of the deletion in the $wnt5^{400}$ allele are schematically shown (**Fig 1i**). In summary, *wnt5* overexpression in the ORNs disrupted the stereotyped structure of the AL and elicited the formation of ectopic glomeruli at the midline.

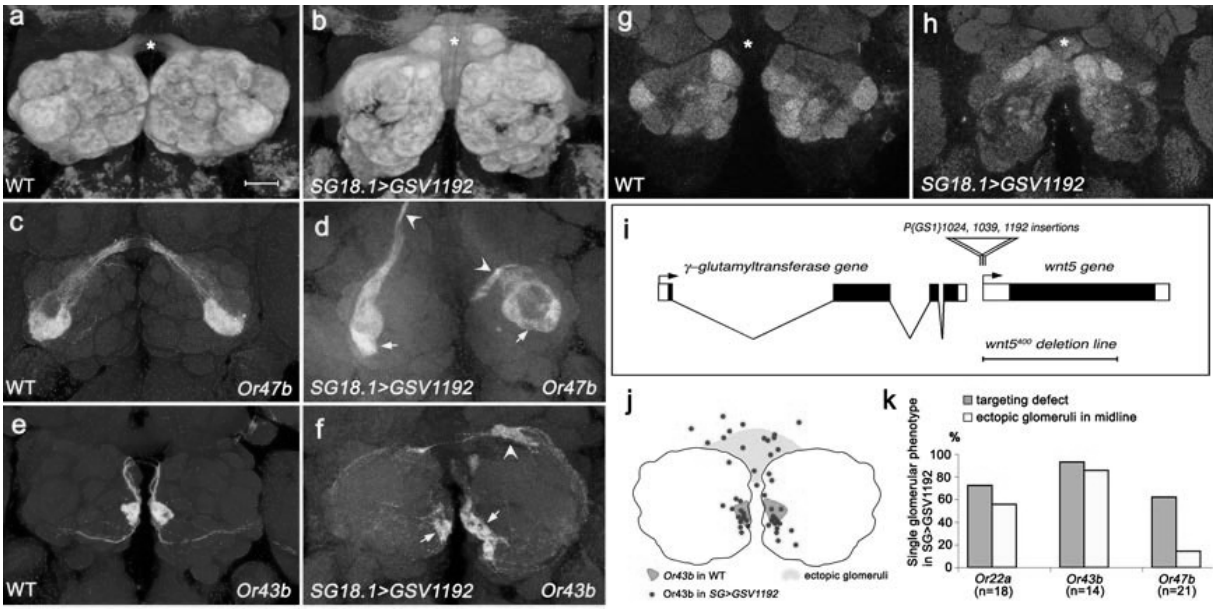

Figure 1. *wnt5* overexpression in the ORNs severely disrupts the organization of glomeruli in the ALs Brains of wild-type (**a, c, e, g**) and *P{GS1}1192* animals (**b, d, f, h**) are shown. ORN axon terminals are visualized with *GFP* under the control of *SG18.1-Gal4* (**a, b**), *Or47b* (**c, d**) and *Or43b* (**e, f**). Postsynaptic PN dendrites are visualized with *GH-mGFP* (**g, h**). The brains are stained with the nc82 (red) and anti-GFP (green) antibodies. (**a**) The wild-type AL is spherical and has a stereotyped arrangement of glomeruli. A commissure connects the left and right ALs (asterisk). (**b**) In the *wnt5*-overexpressing animals, the glomerular arrangement is disrupted and ectopic glomeruli form in the midline (asterisk). (**c**) The *Or47b* glomerulus is normally located on the lateral aspect of the AL. (**d**) In *wnt5*-overexpressing animals the *Or47b* glomerulus is split into multiple parts, which are frequently found at the midline (arrowhead). (**e**) The *Or43b* glomerulus is normally located at the middle edge of the AL. (**f**) In *wnt5*-overexpressing animals it always ectopically project split parts to the midline (arrowhead). (**g**) In the wild type, *GHmGFP* labels a stereotyped pattern of PN dendrites. (**h**) In *wnt5*-overexpressing ALs, the pattern of PN dendrites is disrupted and dendritic processes ectopically enter the midline (asterisks). (**i**) Schematic diagram of the *wnt5* locus showing the positions of the *P{GS}* insertions and the breakpoints of the deletion in $wnt5^{400}$. (**j**) Plots of the positions of *Or43b* in the wild type and the *wnt5*-overexpressing animals. Many of the split glomeruli of *Or43b* are found in the dorsal region of the ALs or in the midline between the ALs. (**k**) Quantification of the frequency of targeting defect or the ectopic glomeruli found in the midline in the *Or22a, Or43b* and *Or47b* subtypes (n = 18, 14 and 21 brains respectively). Scale bar = 20 µm. (see Appendix: Selected Color Figures)

wnt5 is Necessary for the Topographic Organization of the Antennal Lobes

To determine if *wnt5* normally functions in the ALs, we examined the ALs of the $wnt5^{400}$ null mutant, which is homozygous viable[22]. In the wild type expressing GFP under the control of *SG18.1-Gal4*, the bilaterally symmetric ALs were connected by the antennal commissure (**Fig.**

2a). In the *wnt5*^{400} mutant, many ALs (37/55 ALs, ~67%) were not connected by commissures, (**Fig. 2b**). The lobes also appeared misshapen, being flattened dorsally and elongated ventrally, producing a characteristic heart shape (**Fig. 2c, e'-h"**). To investigate the glomerular arrangement in these malformed lobes, we labeled the axonal terminals of 5 subclasses of antennal ORNs and 3 subclasses of maxillary palp ORNs. In the wild type, these glomeruli are located at stereotyped positions in the AL[28,29] (**Fig. 2e-h**). In the *wnt5*^{400} mutant, the dorsal edge of the AL appeared closer to many glomeruli (**Fig. 2d, e'-h'',i**). To test the possibility that the displacement of the dorsal edge is the result of distortions of the AL, we measured the distance between glomeruli in the same AL (*Or47a*, *Or47b*, and *Or67d*; **Fig. h-h", i**). For example, in the wild type the distance between the *Or47a* and *Or47b* glomeruli is 22.51 ± 1.60 µm (n = 32 ALs). In the *wnt5*^{400} mutant this distance decreased to 8.70 ± 2.73 µm (n = 32 ALs; p = 0.0001 compared with wild type). Thus, the dorsoventral distances between glomeruli were reduced in mutant animals (**Fig. 2i**), indicating that the ALs are distorted. These data suggest that a characteristic feature of the *wnt5*^{400} AL is the "collapse" of the dorsomedial corner of the AL. In addition to their shift in positions, a small percentage of glomeruli are also split into smaller subunits (arrowheads, **Fig. 2 e'-h", j**). Examination of the ORN fibers also shows that ORN axons sometimes took meandering paths towards their ipsilateral targets (arrows, **Fig. 2e'-e", f-f'**). Strikingly, the contralateral fibers frequently stall before reaching the commissure (double arrowheads, **Fig. 2h"**), loop back on the ipsilateral glomeruli (double arrowheads, **Fig. 2f", h'**), or project aberrantly to dorsal regions of the brain (**Fig. 3d**). In summary, the loss of *wnt5* resulted in aberrant targeting of the ORN axons and the displacement of many glomeruli. The ventral shift of dorsomedial glomeruli resulted in the ALs acquiring a characteristic heart shape appearance.

We also examined the PN dendrites by expressing GFP under the control of the *GH146-Gal4* driver. In the wild type, *GH146-Gal4* labels a subset of PN dendrites revealing an invariant pattern in the AL neuropil (**Fig. 2k**). In the *wnt5*^{400} mutant this pattern was disrupted, and many dendritic arbors are displaced ventrally (**Fig. 2l**). Thus, mutation of the *wnt5* gene disrupted the targeting of the ORN axons and the positioning of the PN dendrites.

wnt5 Functions in Antennal Lobe Development

To determine when the observed defects arise in the *wnt5*^{400} mutant, we evaluated the AL structure of the *wnt5*^{400} mutant during the pupal stage, a period of significant AL growth and patterning[25,30]. In the control *wnt5*^{400}/+ heterozygote at 26 hours after puparium formation (hAPF), the AL is oval shaped (~35 µm in diameter), and has a smooth neuropil (Fig. 3a). ORN axons have arrived at the outer surface of the ALs, and are also projecting across the midline in a commissure ~5 µm in width. At 50 hAPF, the AL has grown considerably (~55 µm diameter), and the neuropil is well partitioned into glomeruli, which have an adult-like morphology and arrangement (Fig. 3c). Most axons have arrived in the nerve fiber layer, and a thick commissure connects the left and right ALs. In the hemizygous *wnt5*^{400}*/Y* mutant at 26 hAPF, the ALs were oval shaped as in the wild type, although in many brains, axons appeared to project dorsally instead of across the midline (Fig. 3b). At 50 hAPF, further differences between the controls and *wnt5* mutants are seen. The ALs had shifted ventrally with respect to the mushroom body. They were also misshapen; many showing the distinctive heart shape seen in the adult (Fig. 3d). Contralateral axons failed to decussate, instead projected dorsally in 85% of the brains examined at this stage (22/26, Fig. 3e). In the remainder, contralateral axons traverse normally across the midline. By the adult stage, the proportion of mutant brains which had no commissures remains high (67%, 37/55 brains), although many of the brains no longer showed dorsal projections, indicating that the dorsally

projecting axons have likely retracted or degenerated (Fig. 3e). These results indicate that *wnt5* is required during development to regulate ORN axon projection and AL development.

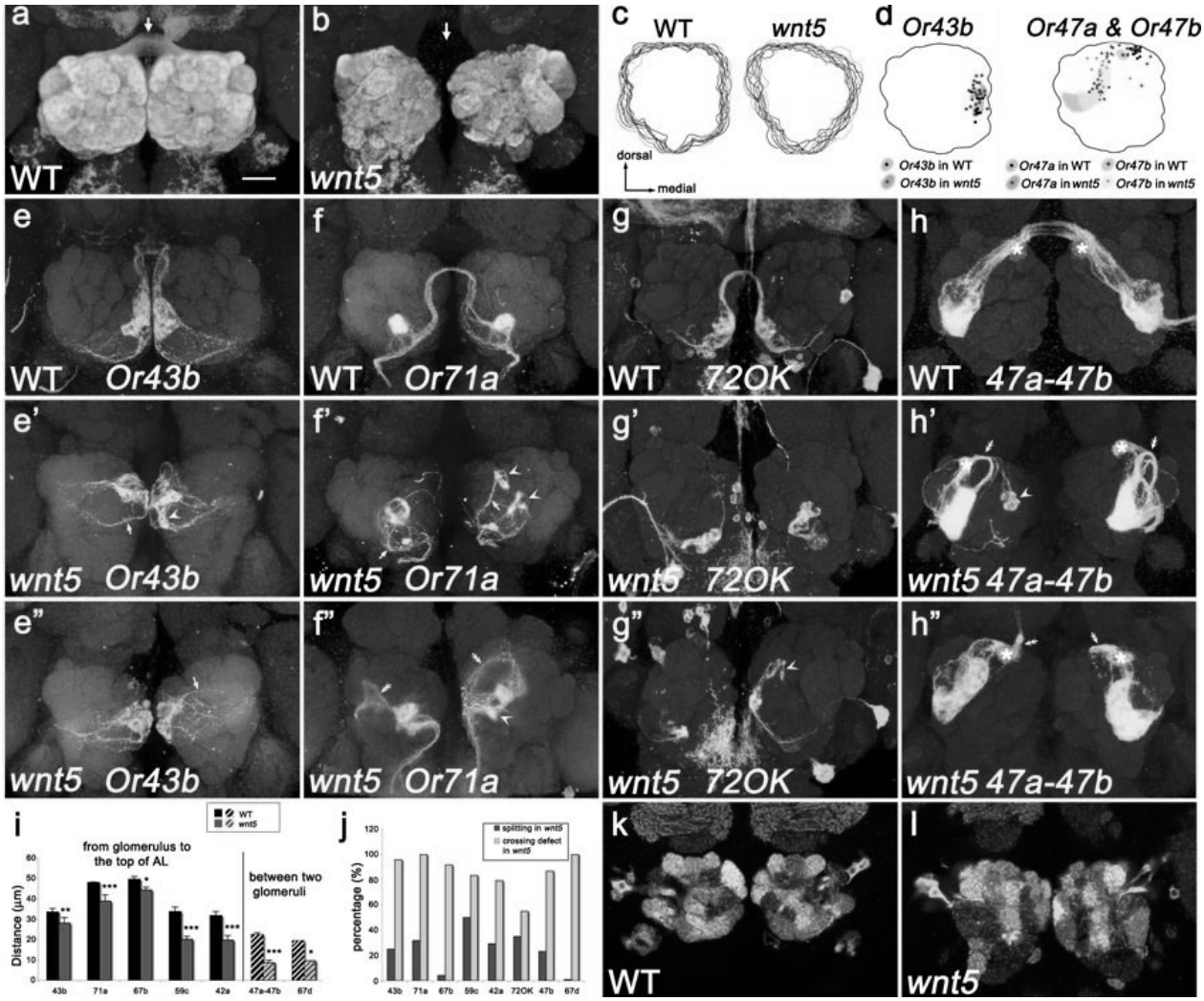

Figure 2. The stereotyped anatomy of the AL is disrupted in the *wnt5* mutant Preparations of wild type (**a, e, f, g, h, k**) and $wnt5^{400}$ mutant (**b, e', e", f', f", g', g", h', h", l**) ALs are shown. ORN axons (glomeruli) are visualized by expressing GFP under the control of various Gal4 drivers. (**a**) Wild-type ALs expressing GFP under the control of SG18.1-Gal4 are spherical and are connected by a commissure (arrow). (**b**) In the $wnt5^{400}$ mutant, the ALs are misshapen, displaced ventrally, and are often unconnected by the commissure. (**c**) Superimpositions of the outlines of ALs from wild type and the $wnt5^{400}$ mutant (n = 12 for each). Dorsal is up and the lateral is to the left. The $wnt5^{400}$ mutant ALs are flattened dorsomedially giving them a characteristic heart-shape appearance. (**d**) Plots of the positions of three different glomeruli in the wild type and the $wnt5^{400}$ mutant. The positions of the Or43b and Or47b glomeruli are shifted more dorsally, while that of the Or47a glomerulus is shifted more ventrally. (**e-g**) Wild-type ALs in which single glomeruli are labeled using UAS-mGFP expressed under the control of the Or43b-Gal4, Or71a-Gal4, and 72OK-Gal4 drivers. The glomeruli are located in their expected positions. (**e', e", f', f", g', g"**) $wnt5^{400}$ mutant ALs with the same highlighted glomeruli. The glomeruli are frequently displaced more dorsally or split into smaller structures (arrowheads). ORN axons also take meandering paths (arrow) to their glomerular targets and fail to cross the midline (double arrowheads). (**h**) Simultaneous labeling of the Or47a (asterisks) and Or47b glomeruli in the wild type showed that they are separated by 22.51 ± 1.6 µm (n = 20). (**h', h"**) In the wnt5400 mutant, the distance between the Or47a (asterisk) and Or47b glomeruli is reduced to 8.70 ± 2.74 µm (p = 0.0001, n = 26). (**i**) Histograms show the distances from the glomeruli (Or43b, Or71a, Or67b, Or59c, and Or42a) to the top edge of ALs, between the Or47a and Or47b glomeruli, and between the two Or67d glomeruli. In the wnt5400 mutant (red bars), the distances are decreased. (**j**) Quantification of the splitting (blue bars) and midline crossing defects (green bars) observed for the various ORN subclasses in the $wnt5^{400}$ mutant. (**k**) The wild-type AL has a characteristic arrangement of PN dendritic arbors, labeled by GH164-Gal4 driving UAS-mGFP. (**l**) In the wnt5400 mutant, the invariant pattern is not seen indicating that the dendritic patterning is disrupted. Scale bar is 20 µm.

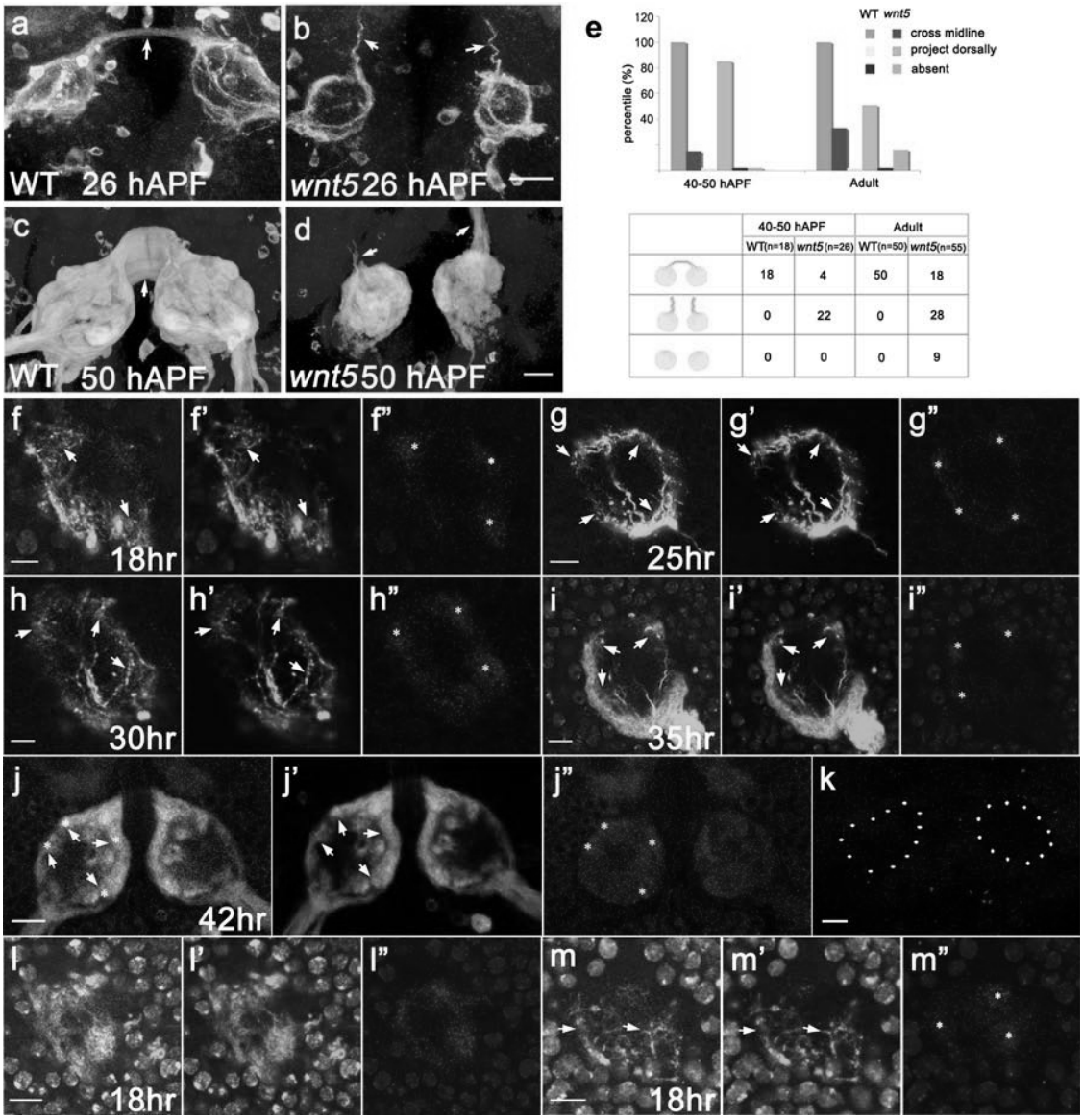

Figure 3. Wnt5 functions during AL development and localizes to PN dendrites The ALs of control (**a, c, f, h**), *wnt5*^{400}/Y hemizygous (**b, d**) and *drl2* homozygous animals (**g, i**), expressing SG18.1-Gal; UAS-mGFP **(a-d**) or GH146-Gal4; UAS-mGFP (**f-i**) were stained with nc82 (red) and anti-GFP (green) to visualize the AL neuropil and GFP, respectively. (**a**) At 26 hAPF, ORN axons in the control animal have arrived at the AL surface and begun to cross the midline in a thin commissure (arrow). The AL neuropil has a smooth texture. (**b**) In the wnt5400 mutant at 26 hAPF, ORN axons have also reached the ALs. However, the axons fail to cross the midline, and instead project dorsally (arrows). (**c**) At 50 hAPF, the AL of the control is partitioned into distinct glomeruli and the left and right lobes are connected by a thick commissure (arrow). (**d**) In the wnt5400 mutant at 50 hAPF, the ALs are misshapen and the commissure is missing. Instead thick fascicles (arrow) extend toward the dorsal part of the brain.
(**e**) Quantification of the commissural defects seen in the wnt5400 mutant at either 40-50 hAPF or adulthood. (**f**) Pupa brains expressing GFP under the control of pbl-Gal4 (green, **f-j**) are dissected at 18, 25, 30, 35 or 42 hAPF and stained with Wnt5 mAb (red). The Wnt5 protein accumulates in the four spherical structures (asterisks at dorsomedial, dorsolateral, ventromedial and ventrolateral) in the ALs. At 18 hAPF, invading axon terminals are seen surrounding the four regions of enriched Wnt5 staining. (**g** to **i**) ORN axon terminals begin to condense as the nerve fiber layer becomes distinct. The Wnt5 distribution remains unchanged. (**j**) At 42 hAPF, the ORN axons have coalesced into distinct glomeruli, which overlapped with the regions of Wnt5 staining. (**k**) No Wnt5 staining is seen in the wnt5400 mutant brain at 50 hAPF, indicating that it is specific for the Wnt5 antigen. Dotted outlines indicate the positions of the ALs. (**l**) At 18 hAPF, PN dendrites are visualized using GFP (green) under the control of GH146-Gal4 and show significant colocalization with regions of Wnt5 enrichment (red). (**m**) At 18 hAPF, brains overexpressing UAS-wnt5 and GFP (green) in the axon terminals under the control of pbl-Gal4 show similar Wnt5 (red) staining pattern, suggesting Wnt5 does not accumulate in the ORN axons even when forcibly expressed in the cells. All scale bars are 20 μm in length. (see Appendix: Selected Color Figures)

Wnt5 Protein is localized in the developing Antennal Lobes

To ascertain the distribution of Wnt5 protein in the olfactory system, we stained developing brains with an anti-Wnt5 antibody[22]. The Wnt5 antibody did not stain *wnt5*^{400} mutant brains (Fig. **3k**), demonstrating its specificity. We first stained animals expressing GFP under the control of *pbl-Gal4*, a pan olfactory neuron driver31. We focused on the pupal stage, when AL defects first become apparent in the *wnt5*^{400} mutant. We observed ORN axons penetrating into the AL as early as 18 hAPF, (arrows, **Fig. 3f**). At this time Wnt5 immunolabeling was seen in four spheroidal structures (~7 μm in diameter) located at the dorsomedial, dorsolateral, ventromedial and ventrolateral regions of the AL; each was surrounded by masses of axonal terminals (asterisks, **Figs. 3f-f'**). This pattern of Wnt5 expression remained relatively unchanged up to 35 hAPF (**Fig. 3g-i**). Comparison of the regions of Wnt5 staining with the regions of GFP staining showed that Wnt5 was located within the space circumscribed by the nerve fiber layer (**Fig. 3i**). At 42 hAPF, as ORN axons are coalescing to form glomeruli, the niduses of axonal terminals overlapped with the regions of Wnt5 accumulation (**Fig. 3j**). To identify the spheroidal structures, we stained 18 hAPF animals expressing GFP under the control of *GH146-Gal4*, which labels the PN dendrites. Wnt5 immunoreactivity largely coincided with the PN dendrites, indicating that Wnt5 is localized to PN dendrites during the period of glomerular development (**Fig. 3l**). We show below that *wnt5* functions in the ORNs. To determine if forcible expression of *wnt5* in ORNs would lead to colocalization of Wnt5 protein with the ORN axon terminals, we stained animals expressing *UAS-wnt5* under the control of the *pbl-Gal4* driver. In these animals, Wnt5 was found in a pattern indistinguishable from that of wild type (**Fig. 3m**), indicating that Wnt5 does not accumulate in the ORN axon terminals. Besides the dendritic localization, we show below that Wnt5 also accumulated in the region of the antennal commissure in the *drl*^{2} mutant (**Fig. 9g**). Wnt5 staining was greatly reduced by 70 hAPF, when glomerular development is largely complete (data not shown). Our immunolocalization result indicates that Wnt5 is localized to the incipient glomeruli during the period of ORN axon targeting and glomerular development.

wnt5 is Required in the Olfactory Receptor Neurons

To delineate the cell type in which *wnt5* functions, we first restored *wnt5* function to specific cell types in the *wnt5*^{400} mutant background. We employed a *UAS-wnt5* transgene[22], which expresses *wnt5* at a low level and therefore does not disrupt AL development (**Supplementary Fig. 1**). Three criteria were specifically assessed: the shape of the AL, the position of the *Or47b* glomerulus, and the presence or absence of the commissure. In the *wnt5*^{400} mutant the AL was heart shaped (compare **Figs. 4a, b**), the *Or47b* glomerulus was located 14.44 ± 0.8 μm from the dorsal edge of the AL compared with 24.66 ± 1.3 μm in the wild-type ($p < 0.0001$, $n = 14$; **Figs. 4e, g**), and the commissure is present in only 30% of the brains. When we expressed *UAS-wnt5* using the *GH146-Gal4* driver, which is expressed in PNs, the mutant phenotype was not rescued, but instead was exacerbated as evidenced by the severe distortion of the ALs and disruptions in the position of the *Or47b* glomerulus (**Fig. 4h**). No rescue was also observed when *UAS-wnt5* was expressed under the control of *MZ317-Gal4*, which is expressed in glia (data not shown). When *UAS-wnt5* was expressed under the control of *SG18.1-Gal4*, the *wnt5*^{400} mutant phenotype was significantly rescued. The rescued ALs were spherical, instead of heart-shaped (**Fig. 4c, f**), the *Or47b* glomerulus was located 20.12 ± 1.4 μm from the dorsal edge of the AL ($p = 0.0102$ compared with mutant, $n = 24$; **Figs. 4e, g**), and the ALs were connected by a commissure in 55% (11/20) of the brains. Expression of *UAS-wnt5* under the control of the *72OK-Gal4* driver, which is expressed in a subset of ORNs[8], also significantly rescued the mutant phenotype. The rescued ALs had a wild-type shape (**Fig. 4d, f**), the *Or47b* glomerulus was located 19.68 ± 1.2

µm from the dorsal edge of the AL (p = 0.001 compared with mutant, n = 16; **Figs. 4e, g**), and the ALs were connected by a commissure in 77% (10/13) of the brains.

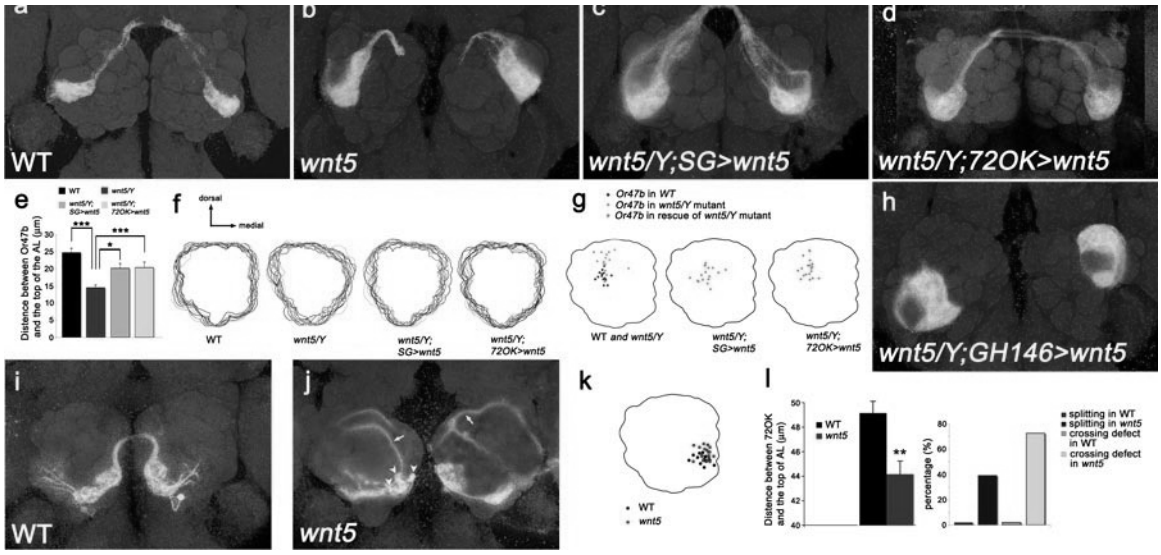

Figure 4. wnt5 functions in the Olfactory Receptor Neurons Preparations of wild-type control (**a**) *wnt5*^{400} mutant (**b**) and rescued wnt5400 mutant ALs (**c, d**). (**a**) In the wild type, the ALs are roughly spherical and the Or47b glomerulus (labeled using the Or47b-mGFP transgene) is located stereotypically in the lateral region of each AL. (**b**) In the *wnt5*^{400} mutant, the ALs exhibit a characteristic heart-shaped morphology and the Or47b glomeruli are displaced towards the dorsal part of the ALs. (**c**) The wnt5 mutant phenotype is rescued by the expression of UAS-wnt5 using the SG18.1-Gal4 driver. (**d**) The wnt5 mutant phenotype is also rescued by the expression of UAS-wnt5 using the 72OK-Gal4 driver. The Or47b glomerulus is identified through its distinctive crescent shape and outlined. (**e**) Histograms show the distances between the Or47b glomerulus and the top edge of the AL in the various genotypes. (**f**) Superimpositions of the outlines of ALs from various genotypes (n = 12 for each). The *wnt5*^{400} mutant ALs have a characteristic heart shape. Expression of UAS-wnt5 using the SG18.1-Gal4 and 72OK-Gal4 drivers rescued the wnt5 mutant ALs to the wild-type shape. (**g**) Plots showing the positions of the Or47b glomerulus in the various genotypes. The Or47b glomerulus is displaced more dorsally in the *wnt5*^{400} mutant. Expression of UAS-wnt5 using the SG18.1-Gal4 and 72OK-Gal4 drivers moves the Or47b glomerulus ventrally to the wild-type position. (**h**) The wnt5 mutant phenotype is not rescued by the expression of UASwnt5 using the GH146-Gal4 driver. (**i**) In ALs with wild-type clones, the 72OK glomerulus is located in the ventromedial part of AL and is connected with the contralateral glomerulus by a distinct fascicle that crosses midline. (**j**) In ALs carrying *wnt5*^{400} mutant clones, the 72OK glomerulus is split into smaller structures (arrowheads) and contralateral axons fail to cross the midline and instead loop back (arrows) on the ipsilateral glomerulus. (**k**) A plot of the positions of the 72OK glomerulus showing that it is displaced slightly dorsally in the wnt5400 mosaic animal. (**l**) Quantification of the distance between the 72OK glomerulus and the top edge of the AL, the splitting of glomerulus, and the absence of the contralateral tract, in the wild-type and wnt5 mosaic animal. SG = SG18.1-Gal4; 72OK = 72OK-Gal4. Scale bar is 20 µm. (see Appendix: Selected Color Figures)

Next, we investigated whether *wnt5* is required in the ORNs for proper AL development. We employed the MARCM system[32] to generate *wnt5* mutant ORNs in otherwise wild-type background. We induced and examined clones of wild-type or *wnt5*^{400} homozygous *72OK* cells. Large clones were examined since small clones were likely to be rescued by Wnt5 secreted from wild-type tissues adjacent to the clones, as was indeed observed (data not shown). In control animals with wild-type clones, the ALs had a spherical shape (**Fig. 4i**). The wild-type *72OK* ORNs projected to their expected positions (49.14 ± 3.5 µm from dorsal surface of AL, n = 14, **Fig. 4k, l**) and form glomeruli with stereotyped shapes. Their contralateral axons formed a distinct fascicle that project normally across the midline. In animals bearing *wnt5*^{400} clones, the ALs were misshapen, with a heart-shaped appearance (**Fig. 4j**). The mutant *72OK* ORNs projected to a slightly more dorsal position compared to that of the control (44.16 ± 4.5 µm, p = 0.002, n = 18; **Fig. 4k, l**), and formed distorted and split glomeruli (**Fig. 4j, l**). Their contralateral axons frequently appeared defasciculated and often (72.2%, 13/18 brains) failed to project across

the midline (**Fig. 4j, l**). Our cell-type specific cDNA rescue and mosaic experiments therefore indicated that *wnt5* was required in the ORNs for appropriate AL patterning.

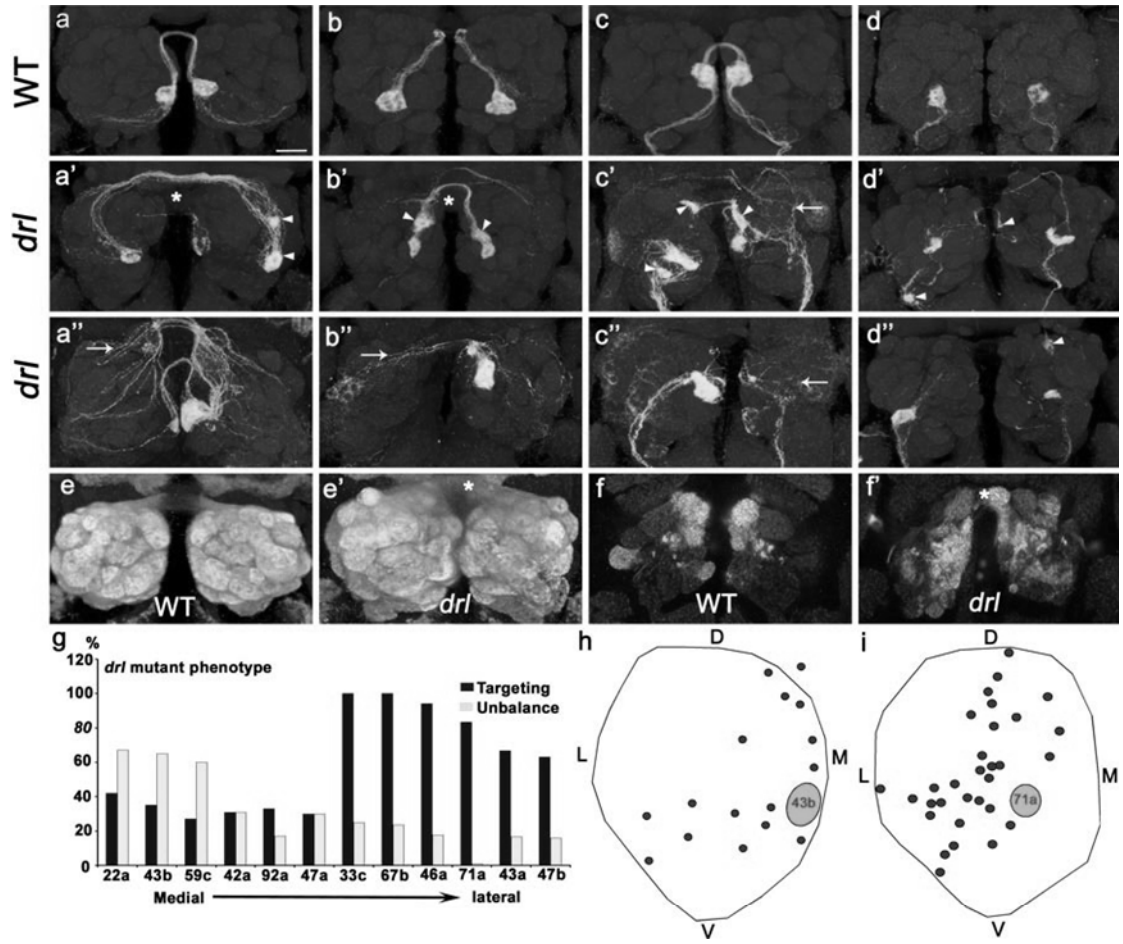

Figure 5. The stereotyped anatomy of the AL is disrupted in the *drl* mutant Preparations of wild type (**a-f**) and drl^2 mutant (**a'-f'**) are shown. ORN axons and PN dendrites are labeled by expressing GFP under the control of various *Gal4* drivers. (**a-d**) In the wild type, the *Or43b, Or67b, Or42a, and Or71a* glomeruli have specific shapes and are located in their predicted positions. (**a'-d"**) In the drl^2 mutant, the glomeruli are often split into smaller structures (arrowheads, **a'-d', d"**) and localized to ectopic positions. They are also often missing from one side (**a"-c"**). In addition, ORN axons take circuitous routes to their targets (arrows, **c', a"-c"**). (**e-e'**) The ALs are visualized by SG-Gal4 driving GFP expression. (**e**) The wild-type ALs are spherical and connected by a commissure. (**e'**) In the drl2 mutant, ectopic protrusions can be seen at the midline (asterisk). (**f-f'**) Dendritic arbors are visualized by expressing GFP under the control of *GH146*-Gal4. (**f**) In wild type, a deep section at the level of the commissure shows that dendritic arborization do not enter the midline. (**f'**) An equivalent section in the drl2 mutant, showing that the dendritic arbors have invaded the midline (asterisk). (**g**) Quantification of the "targeting" (blue bars) or the "unbalanced" (yellow bars) defects in the various ORN subtypes. The ORN subtypes are arranged from medial (left) to lateral (right). While all glomeruli show both defects, the "unbalanced" defect predominates among the medial glomeruli. Plots of the positions of the ectopic (**h**) *Or43b* and (**i**) *Or71a* glomeruli (red circles) in the drl^2 mutant. There appears to be no consistent pattern in the distribution of the ectopic glomeruli. Scale bar is 20 μm. n ≥ 15. (see Appendix: Selected Color Figures)

drl is Necessary for Patterning the Glomerular Map

The capacity of Wnt5, expressed by the ORNs, to regulate glomerular patterning, focused our attention on its potential downstream signalling pathway. The Derailed (Drl) receptor tyrosine kinase has been shown to act as a receptor for the repulsive Wnt5 cue in axons that cross the embryonic midline in the anterior commissure of each hemisegment[21]. To determine if *drl* also functions in the AL, we examined the ALs of the drl^2 null mutant[33]. In the homozygous mutant

expressing GFP under the control of *SG18.1-Gal4*, the glomerular map appeared deranged (compare **Figs. 5e, e'**). In 39% (22/56) of the mutant brains, ectopic glomeruli developed at the midline (asterisks in **Figs. 5a', b', f'**), while in the remainder (61%), abnormal protrusions extended from the dorsal-medial corner of the ALs. To better assess alteration to the glomerular pattern, we analyzed 7 subclasses of antennal ORNs and 5 subclasses of maxillary palp ORNs. A number of defects were seen in the *drl*^{2} mutant. Many glomeruli were positioned ectopically or split into smaller structures (arrowheads, **Figs. 5a'-d', d"**). Plotting the positions of the *Or43b* and *Or71a* glomeruli in different ALs, revealed no consistent pattern, indicating that the glomeruli were randomly situated in the mutant (**Figs. 5h, i**). Glomeruli ectopically localized to the commissure were seen at low frequencies in all of the ORN subtypes surveyed, suggesting that all subtypes have equal tendency to enter the midline. Some glomeruli are greatly reduced in size or entirely missing from one AL (**Figs. 5a"-c"**). In addition to the glomerular defects, ORN axons frequently take circuitous routes to their targets (arrows, **Figs. 5c', a"-c"**). Strikingly, a number of axons terminate unilaterally (confirmed by unilateral antennal ablations, **Supplementary Fig. 2**), resulting in the loss of presynaptic structures from a single AL (**Figs. 5a"-c"**). To better assess the data, we grouped the glomerular positioning and splitting defects as "targeting defects" (**Figs. 5a'-d', d"**) and the unilateral loss (or reduction) of glomeruli as "unbalanced defects" (**Figs. 5a"-c"**). Both types of defects are present in each of the 10 ORN subclasses **(Fig. 5g)**.

We also inspected the organization of the PNs in the *drl*^{2} mutant using the *GH146-Gal4* marker. In the wild-type adult, *GH146-Gal4*-expressing cells send their neurites into the AL, where they arborize in specific glomeruli, creating a pattern of dendritic arbors (**Fig. 6a**). In the *drl*^{2} mutant adult, the organization of the dendritic arbors appeared chaotic (**Fig. 6b**), and a subset of arbors even invaded the midline where they target the ectopic midline glomeruli (**Figs. 5f, f'**). This midline invasion of the PN dendrites is highly reminiscent of the *wnt5* overexpression phenotype. Loss of *drl* therefore, leads to disruption of the glomerular arrangement and midline invasion by PN dendrites.
We examined the ALs of the *drl*^{2} mutant during the pupal stage to determine when the defects arise during development. The PN dendrites of wild type and *drl*^{2} mutant were visualized using the *GH146-Gal4* driver. At 40 hAPF, fine dendritic processes could be seen growing into the *drl* mutant midline, which was not seen in the wild type (**Fig. 6c, d**). Our analyses indicate that the derangement of the AL in *drl*^{2} is apparent as early as 40 hAPF, a period of major AL growth and patterning.

Drl Protein is localized to PN Dendrites and Midline Glial Cells

To ascertain the localization of the Drl protein in the olfactory system, we stained developing brains with an anti-Drl antibody. We first stained animals expressing GFP under the control of *Repo-Gal4*, which labels glial cells. At 30 hAPF, GFP staining is found in a prominent band (~70 μm x 35 μm) located in between and slightly dorsal to the developing ALs (**Fig. 6e**, bracket). This structure is the "transient interhemispheric fibrous ring" (TIFR)[34], a toroidal glial structure lying in the midsagittal plane of the brain. The ventral edge of the TIFR is closely associated with, and bridges the opposite ALs. In more posterior sections, at the level of the antennal commissure, a thick bundle of glial processes is seen to pass from one AL to the other (**Fig. 6f**). The TIFR is strongly stained by the Drl antibody (**Fig. 6e'**). Immunoreactivity is also seen in the bundle of glial processes linking the opposite ALs (**Fig. 6f'**). We next stained brains from animals expressing GFP under the control of *GH146-Gal4*. At 30 hAPF, GFP highlighted the PN cell bodies and their dendritic arbors in the AL neuropil. Drl immunolabeling largely overlapped with the dendritic GFP staining indicating that Drl is expressed by a big subset of the PN dendrites

(**Fig. 6h**). The Drl antibody did not stain the *drl*^{2} null mutant brains demonstrating its specificity (**Fig. 6g**).

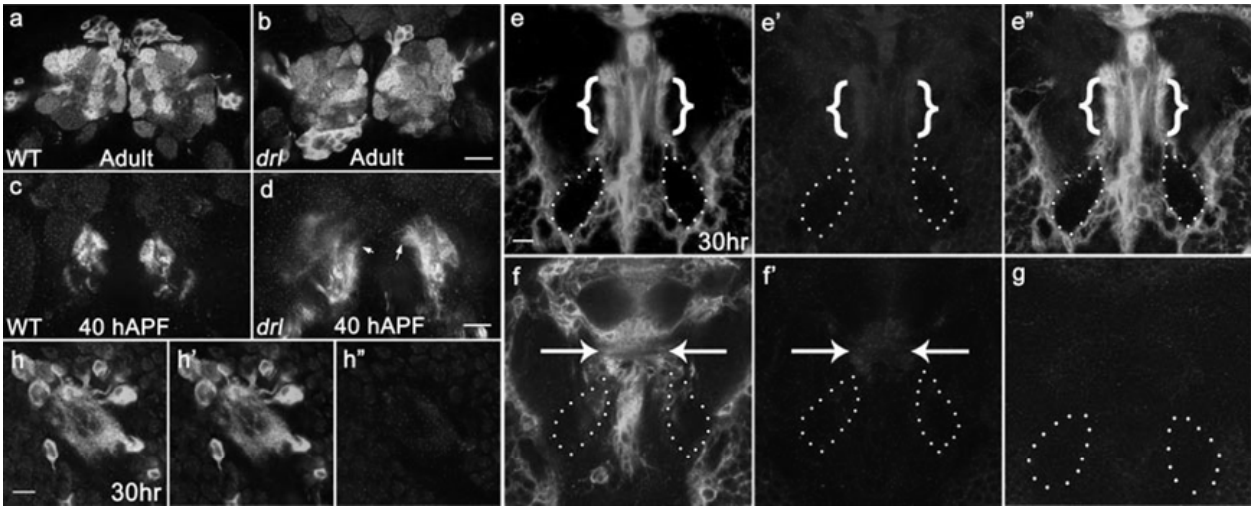

Figure 6. Drl functions during AL development and localizes to TIFR glia (**a**) In the wild-type adult, PNs dendritic arborization is restricted within the confines of the AL. (**b**) An equivalent section in the *drl*^{2} mutant showing that the characteristic pattern is disrupted. (**c**) A optical section of a pair of wild-type ALs at the level of the commissure at 40 hAPF, showing the absence of PN dendrites from the midline region. (**d**) An equivalent section from a *drl*^{2} mutant at the 40 hAPF, showing the extension of PN processes towards the midline (arrow). (**e**) Brains of a 30 hAPF pupa expressing GFP under the control of Repo-Gal4. GFP expression is found in a single layer of glia surrounding the ALs (dotted outlines), but more prominently in a large (~70 µm x 35 µm) midline structure (bracket), the TIFR. The TIFR is located between the ALs, and its ventral edge is closely linked with the developing ALs. (**e'**) The Drl antibody strongly stains the TIFR (red). (**e"**) Overlay of figures (e) and (**e'**) showing the overlap between Drl and GFP immunoreactivity. (f, f') An optical section of the same brain in (**e**), at the level of the antennal commissure. A bundle of glial fibers connects the opposite ALs. This bundle of glial processes expresses the Drl protein (arrows). (**g**) The Drl antibody does not stain the *drl*^{2} mutant brain, demonstrating the specificity of the antibody. (**h-h"**) Brains of a 30 hAPF pupa expressing GFP under the control of *GH146*-Gal4 stained with antibodies against GFP (green), Drl (red) and Elav (blue). GFP expression is found in the dendrites of the PNs, and colocalizes with the Drl staining. For the panels from **a** to **d** and **g** to **i**, the dorsal is to the up and the lateral is to the right. Scale bars are 10µm for a to j Scale bar in k is 20 µm for k-m (see Appendix: Selected Color Figures)

drl Functions in Glial Cells

To delineate the cell types in which *drl* functions, we sought to restore *drl* function to specific cell types in the *drl*^{2} mutant background. Since Drl localized, in part, to PN dendrites, we hypothesized that *drl* acts in the PNs to receive a *wnt5* signal from the ORNs. We employed the *GH146-Gal4* driver, which is active in two thirds of all PNs[35,36], to drive the expression of *UASdrl*. Several criteria were examined to assess genetic rescue: the presence or absence of ectopic midline structures, and the position and integrity of the *Or22a*, *Or43b*, *Or46a*, and *Or47b* glomeruli (**Figs. 7a-d**). In the *drl*^{2} mutant, 100% of the brains showed aberrant midline structures (either midline glomeruli or protrusions) and 38%-94% of the brains showed defects in the positioning or integrity of the glomeruli (**Figs. 7e-h, v**). Expression of *UAS-drl* under the control of *GH146-Gal4* partially rescued the mutant phenotype (58% targeting defects, **Fig. 7t, u, v**).

To determine if *drl* is required in the PNs, we generated and examined *drl* mutant PN MARCM single-cell clones. Loss of *drl* from PNs however, did not disrupt the PN dendrite morphology, or the stereotyped arrangement of the glomeruli in the ALs (**Supplementary Fig. 3**). To further evaluate if *drl* functions in neurons during AL development, we expressed *UAS-drl* under the control of *elav-Gal4*, a pan-neuronal driver. Expression of *UAS-drl* with *elav-Gal4* did not rescue the *drl*^{2} mutant phenotype (data not shown). Next, we tested whether expression of *drl* in glia

would rescue the *drl*[2] phenotype. Expression of *UAS-drl* under the control of the pan-glia driver, *Repo-Gal4*, completely eliminated the midline defects (0%) and significantly reduced the occurrence of targeting defects to 11%-24% for different glomeruli (**Fig. 7i-l, v**). This result suggests that *drl* functions in the glia for the proper development of the ALs.

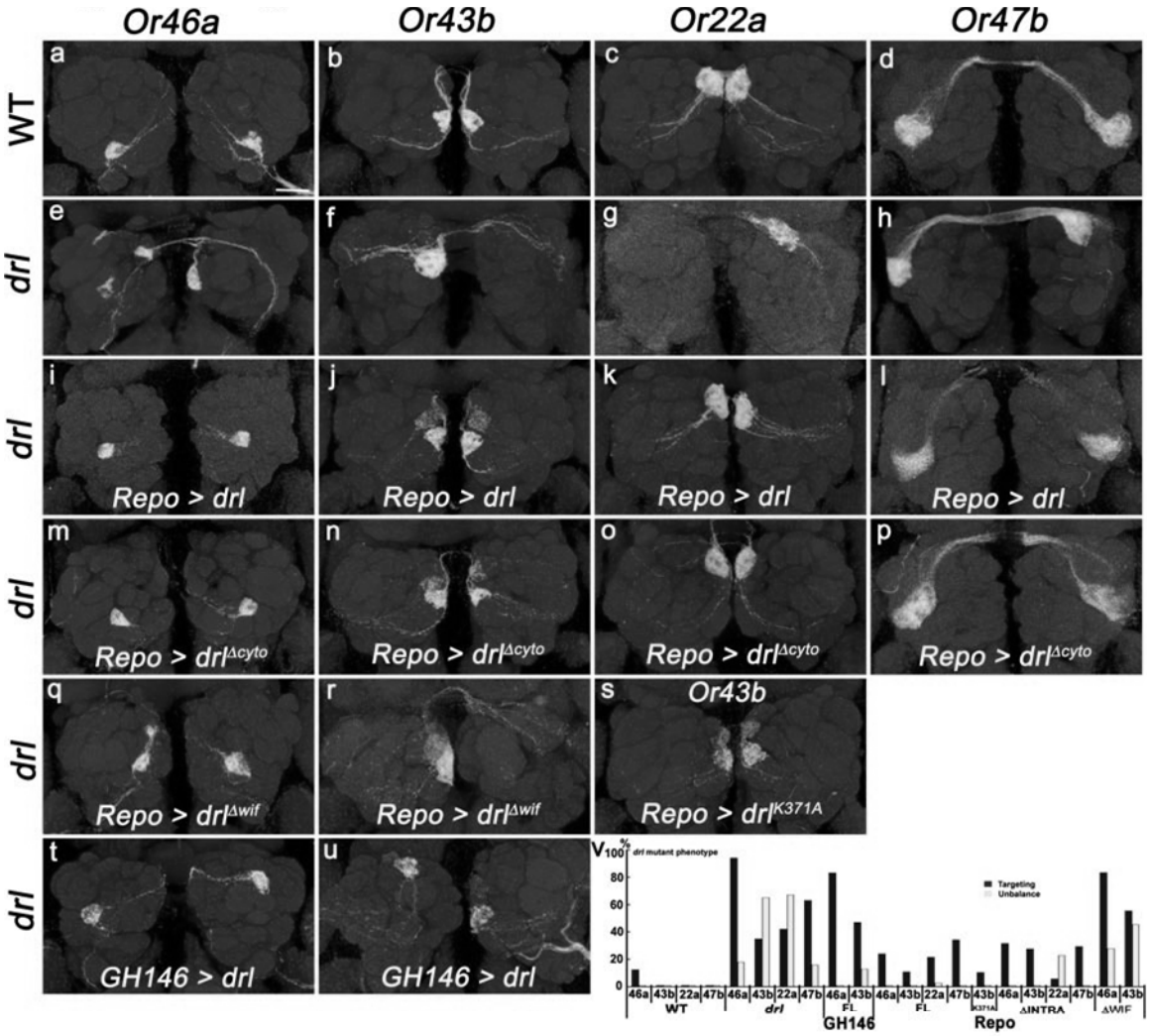

Figure 7. Drl Functions in Glial Cells and its WIF domain is Essential Preparations of wild type (**a-d**) and *drl*[2] mutant, expressing *Or46a-mGFP, Or43b-mGFP, Or22a-mGFP, and Or47b-mGFP* are shown. (**a-d**) Glomeruli have predictable shapes and are located in invariant topographic positions in the wild type. (**e-h**) In the *drl*[2] mutant, glomeruli are ectopically positioned, split, or missing. (**i-l**) Expression of *UAS-drl* under the control of the *Repo-Gal4* driver strongly rescues the mutant phenotype. Glomeruli are located in their stereotyped positions. (**m-p**) Expression of a truncated Drl protein lacking the cytoplasmic domain using the *Repo-Gal4* driver rescues the mutant phenotype. (**q, r**) Expression of a truncated Drl protein lacking the extracellular WIF domain fails to rescue the mutant phenotype. Glomeruli are split, or missing. (**s**) Expression of a "kinase-dead" Drl protein (K371A) also rescues the mutant phenotype. (**t, u**) Expression of *UAS-drl* under the control of *GH146*-Gal4 partially rescues the mutant phenotype. Although the glomerular defects remained, protrusions from the ALs are absent. (**v**) Quantification of the mutant defects found in the various genotypes. Blue bars represent "targeting" defects while yellow bars represent "unbalanced" defects. Scale bars is 20 μm. n ≥ 15. (see Appendix: Selected Color Figures)

Drl Regulates Glomerular Patterning largely through its Extracellular Domain

Our ability to rescue the mutant phenotype provided us with the opportunity to probe the functions of the different domains of the Drl protein in glomerular patterning. Previously it was reported that Drl's cytoplasmic domain is required for its function in embryonic CNS axon pathfinding, although its potential tyrosine kinase activity is dispensable[21]. To determine if the Drl kinase activity is required for AL development, we mutated the conserved K371 residue, which

is essential for kinase activity[38], to an alanine. Expression of the UAS-drlK371A transgene using Repo-Gal4 significantly rescued the *drl* mutant phenotype (26% midline defects, 11% *Or43b* axon targeting defects, compared with 100% midline defects and 35% targeting defects in the drl^{2} mutant, **Fig. 7s**), indicating that kinase activity is not essential for Drl function in AL development. To ascertain if the cytoplasmic domain is needed for AL development, we employed the *UAS-*$drl^{\Delta cyto}$ transgene[39], which encodes a truncated Drl protein bearing only the extracellular and transmembrane domains. Interestingly, *UAS-*$drl^{\Delta cyto}$ retained the ability to rescue the *drl* mutant phenotype (33% midline defects, 23% targeting defects, **Fig. 7m-p, v**). To determine if the Drl WIF domain is needed for AL development, we generated a *UAS-*$drl^{\Delta WIF}$ transgene, which encodes a Drl protein lacking only the WIF domain. The loss of the WIF domain abolished the ability of *drl* to rescue the mutant phenotype (89% midline defects, 56% targeting defects, **Fig.7q, r, v**). Taken together, these results indicate that Drl regulates AL development largely through its Wnt5-binding WIF domain.

wnt5 Functions Downstream of drl to Regulate AL Patterning

We next investigated the genetic relationship between wnt5 and drl. The similarity of the midline defects seen in the *drl* loss-of-function and *wnt5* gain-of-function mutants suggested that these two genes might act antagonistically in AL development. We hypothesized that *drl* might counteract the effect of *wnt5* in regulating the pathfinding of ORN axons. This hypothesis makes the prediction that removal of *drl* would increase the effect of *wnt5*. To test this idea, we examined the effect of expressing a low level of *wnt5* in the drl^{2} mutant background. Expression of a single copy of *UAS-wnt5* under the control of *SG18.1-Gal4* in the wild-type background did not alter the AL structure (Figs. 8c, f, S1). In the drl^{2} mutant, midline glomeruli were found in 39% of the animals, most showing only protrusions from the dorsomedial corner of the ALs (Figs. 8a, d). In contrast, expression of a single *UAS-wnt5* in the drl^{2} mutant background resulted in the induction of large midline glomeruli in 83% of the animals (Figs. 8b, e). Thus *wnt5* function is dramatically increased in the drl^{2} mutant background, consistent with the hypothesis that *drl* antagonizes *wnt5* during glomerular development and AL patterning.

To determine the hierarchical order of *wnt5* and *drl* functions during AL development, we constructed animals bearing null mutations in both genes. We labeled the axon terminals of the *Or47b* ORNs and stained the ALs with the nc82 antibody to assess the glomerular pattern and evaluate AL shape. Heterozygosity for drl^{2} had no effect on the homozygous $wnt5^{400}$ ($wnt5^{400}/Y;$ $drl^{2}/+$) mutant phenotype (data not shown). In contrast, heterozygosity for $wnt5^{400}$ dramatically suppressed the homozygous drl^{2} mutant phenotype ($wnt5^{400}/+;$ drl^{2}/drl^{2}, **Figs. 8i, k**). Suppression of both the dorsomedial AL protrusions (**Fig. 8o, q**) and the glomerular defects typical of the drl^{2} mutant (**Fig. 8i, k**) was observed. Homozygosity for both the $wnt5^{400}$ and drl^{2} null mutations resulted in ALs which exhibited the characteristic *wnt5* mutant phenotype ($wnt5^{400}/Y;$ drl^{2}/drl^{2}, **Fig. 8h, i, j**). The dorsal-medial region of the ALs was collapsed, producing a heart-shaped appearance (**Fig 8n, o, p**) and the *Or47b* contralateral axons failed to cross the midline in 56% of the animals (compared with 100% in drl^{2} mutant and 62% in $wnt5^{400}$ mutant; **Figs. 8j, l**). $wnt5^{400}$ is thus epistatic to drl^{2}, strongly suggesting that *wnt5* functions downstream of, and is repressed by *drl* in the signalling pathway regulating glomerular development.

Wnt5 Protein Accumulates at the Midline in the drl Mutant

The antagonistic relationship between drl and wnt5 posed the question of how they might function together to regulate AL development. The strong midline defects of the *wnt5* and *drl* mutants together with the localization of Drl protein to the TIFR glial processes associated with

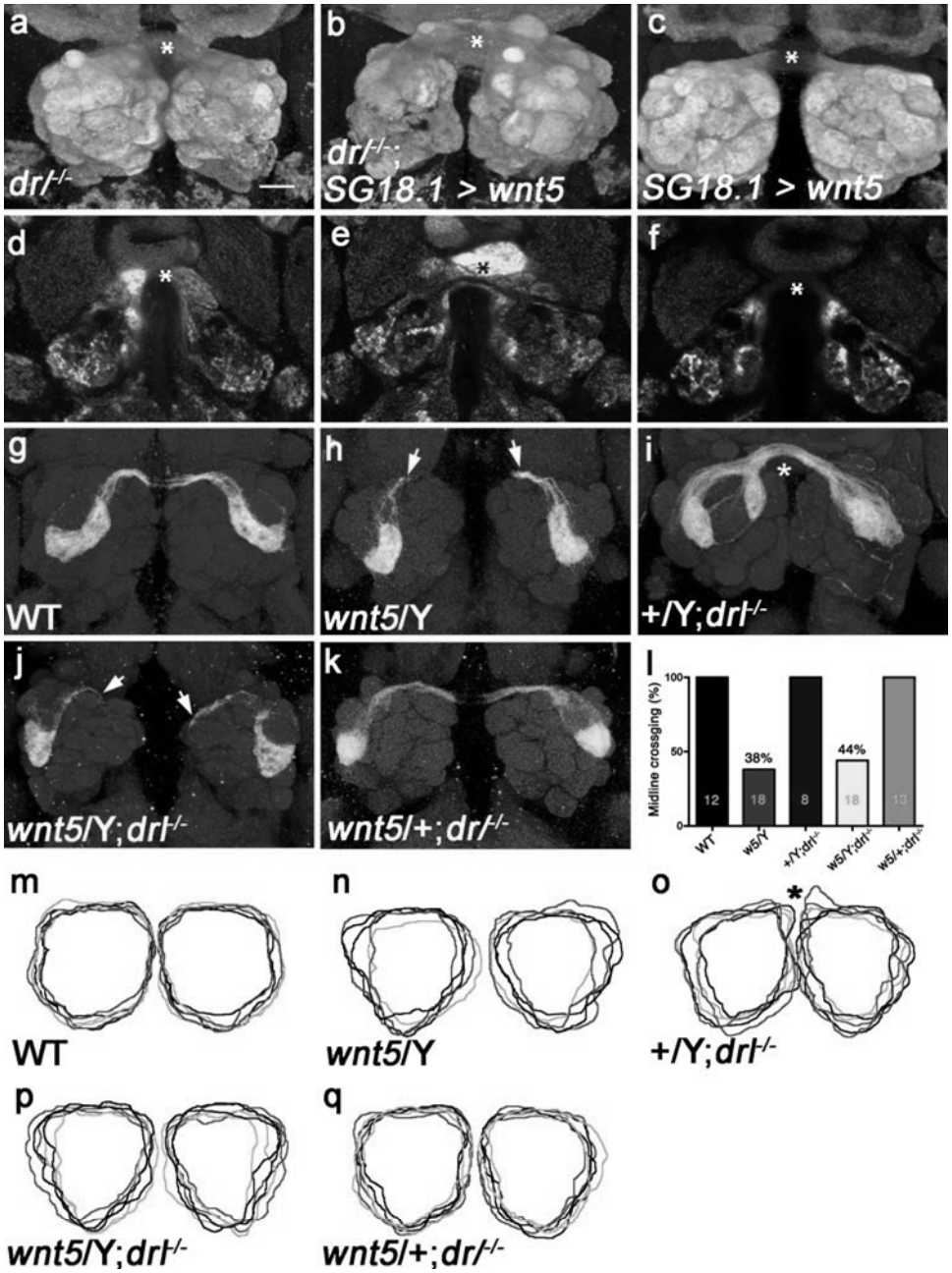

Figure 8. drl functions upstream of wnt5 and to inhibit wnt5 function In panels **a-f**, glomeruli are labeled by expressing GFP (green), under the control of *SG18.1Gal4*. (**a**) ALs of the *drl*^{2} mutant. (**b**) ALs of a *drl*^{2} mutant expressing a *UAS-wnt5* transgene under the control of SG18.1-Gal4. Note the dramatic induction of midline glomeruli (asterisk). (**c**) ALs of a wild-type animal expressing UAS-wnt5 under the control of SG18.1-Gal4. (**d, e, f**) Corresponding deep sections of (**a, b, c**) revealing the more severe midline phenotype of **b**, **e** compared with **a**, **d**. (**g**) Wild-type ALs showing the stereotyped structure and position of the Or47b glomeruli. (**h**) The wnt5400 mutant showing the characteristic wnt5 phenotype: Or47b axons fail to cross the midline (arrow) and the ALs have a characteristic heart-shape appearance. (**i**) The *drl*^{2} mutant showing the characteristic *drl* phenotype: the Or47b glomerulus is split and ectopic glomeruli appear at the midline (asterisk). (**j**) In the wnt5; drl double mutant, results in a characteristic wnt5 phenotype. The ALs have a distinctive heart-shaped appearance and the contralateral fibers of the Or47b axons fail to cross the midline (arrow). (**k**) Removal of a copy of *wnt5* dramatically suppressed the drl mutant phenotype. Ectopic midline structures are suppressed and the overall shape of the ALs become wild-type. (**l**) Quantification of the percentage of ALs showing the failure of Or47b axons to cross the midline. (**m-q**) Superimpositions of the outlines of ALs from the various genotypes (n = 6 for each genotype). ALs from the wnt5 single mutant, and the *wnt5*; *drl* double mutant have a characteristic heart shape, while ALs from the drl mutant have protrusions at the midline (asterisk). Scale bar is 20 μm. (see Appendix: Selected Color Figures)

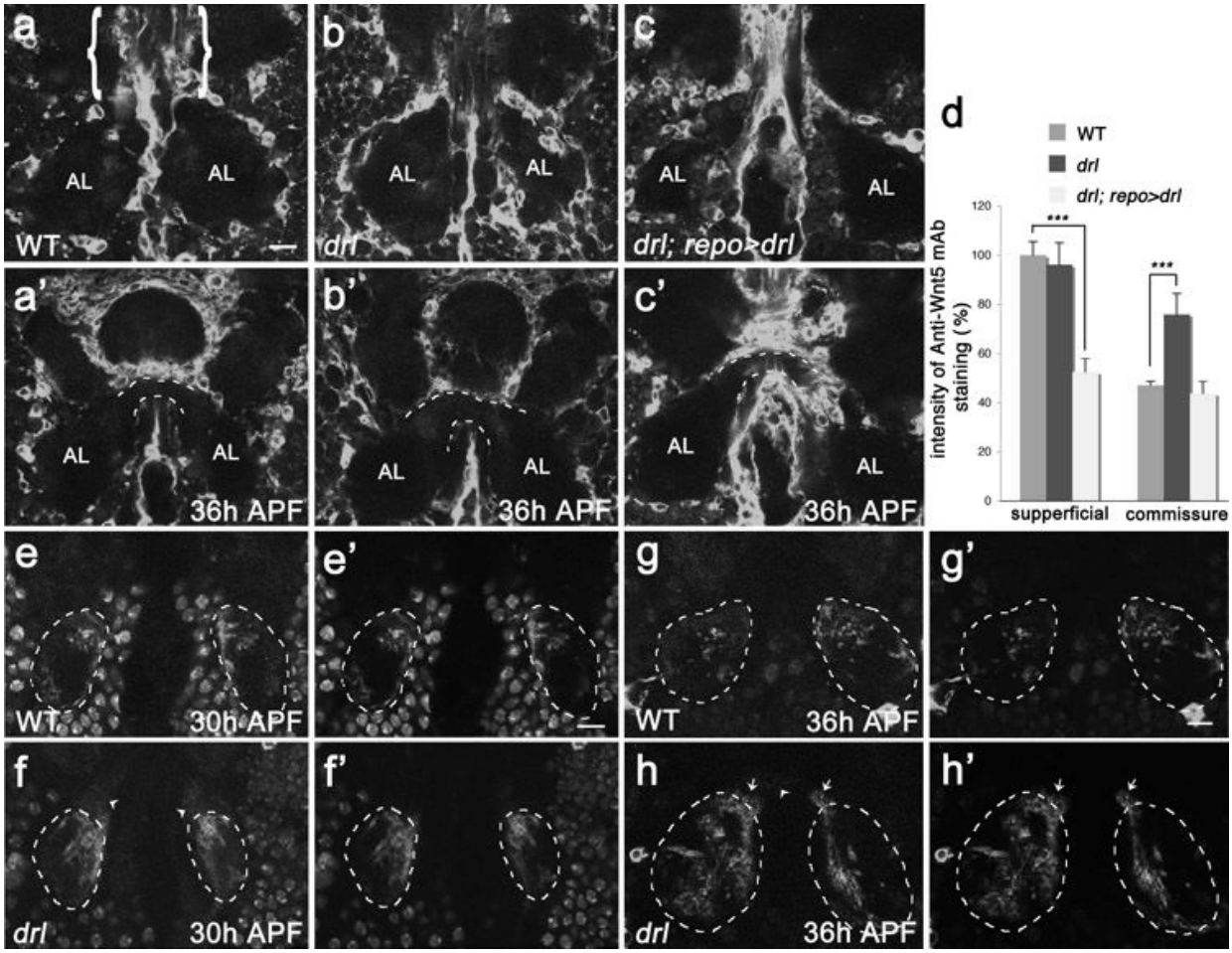

Figure 9. Wnt5 is localized in the AL neuropil and midline commissure in the *drl* mutant animals. Brains of 36 hAPF pupae of wild type (**a, a'**), *drl*^{2} homozygous (**b, b'**) and *Repo-Gal4* driving UAS-drl in the drl2 mutant (**c, c'**) expressing GFP under the control of *Repo-Gal4* were stained with antibodies against Wnt5 (red), GFP (green) and Elav (blue) to visualize the Wnt5 protein, glial cells and neurons, respectively. Anterior optical sections are shown in **a, b** and **c** and posterior optical sections (at the level of the commissure, dashed line) are shown in **a', b**' and **c'**. The TIFR structure is indicated by bracket as in **a**. (**a**) In the wild type, Wnt5 was seen in the AL neuropil, but (**a'**) not detectable in the antennal commissure. (**b**) In the *drl*^{2} mutant, Wnt5 was found in the AL neuropil. (**b'**) Interestingly, Wnt5 is highly enriched in the antennal commissure. (**c**) In drl2 mutant animals expressing *UAS-drl* under the control of *Repo-Gal4*, Wnt5 protein was reduced in both AL neuropil and (**c'**) antennal commissure. (**d**) Quantification of the levels of Wnt5 found in the AL neuropil and commissure of the various genotypes. Brains of wild type (**e, e', g, g'**) and *drl*^{2} mutants (**f, f', h, h'**) expressing GFP under the control of *GH146-Gal4* were stained with antibodies against Wnt5 (red), GFP (green) and Elav (blue) or 36 hAPF (**f-g'**). All the images from **d** to **g'** are the single confocal sections at equivalent posterior level of AL (outlined with dashed lines) to show the antennal commissures. (**e, e'**) A single optical section of the 30h APF wild type brain at the level of the commissure shows that Wnt5 is located along the periphery of the AL neuropil, coincident with the PN dendrites. (**f, f'**) An equivalent optical section of the *drl*^{2} mutant brain at the same stage, showing that Wnt5 is located ectopically, medial to the area occupied by the PN dendrites, and extending towards the midline (arrowheads). (**g, g'**) In the wild type at 36h APF, the expression pattern of Wnt5 remains largely unchanged. (**h, h'**) In the drl2 mutant at this stage, Wnt5 is found ectopically within the antennal commissure (arrowheads). In addition, PN dendrites are now seen to transgress the AL boundary and extend towards the midline (arrows). (see Appendix: Selected Color Figures)

the midline suggests that Drl may regulate Wnt5 there. To investigate the physical association of Wnt5 and the midline glia, we examined the localization of the Wnt5 protein in wild-type pupae expressing GFP under the control of the *Repo-Gal4 driver*. As mentioned above, we observed Wnt5 immunoreactivity in the AL neuropil at 36 hAPF (Figs. 9a, d, 100 ± 5.5%, n = 8 ALs). However, we did not observe significant Wnt5 immunostaining in the antennal commissure in the wild type at this time (Fig. 9a', 47.0 ± 1.7%, n = 8 ALs). Next, we stained for the Wnt5 protein in the *drl*^{2} loss-of-function mutant. As in the wild type, Wnt5 is found in the AL neuropil

in the drl^{2} mutant (Figs. 9b, d, 96.0 ± 8.9%, n = 16 ALs). Strikingly, a large amount of Wnt5 is also found in the antennal commissure, a structure enwrapped by processes of the TIFR glia (dashed lines, Fig. 9b', 75.9 ± 8.5%, n = 16 ALs, $p < 0.0001$ compared with wild type commissure). This result indicates that, in the wild type, *drl* downregulates Wnt5 protein in the antennal commissure. To determine if the downregulation of Wnt5 at the midline is due to *drl* acting in glia, we restored *drl* specifically to glia in the drl^{2} mutant. In drl^{2} mutants expressing *UAS-drl* under the control of the *Repo-Gal4* driver, Wnt5 staining in the antennal commissure was no longer observed (Figs. 9c', d, 43.7 ± 4.7%, n = 16 ALs, p = 0.25).

The ectopic midline expression of Wnt5 in the drl^{2} mutant prompted us to ask how the commissural Wnt5 might affect glomerular development in the mutant. To address this question, we visualized the development of the PN dendrites in the *drl* mutant by expressing GFP under the control of *GH146-Gal4*. At 30 hAPF, as Wnt5 began to accumulate in the dorsomedial corners of the ALs in the drl^{2} mutant (arrowheads in **Figs. 9e and f**), the PN dendrites were seen lateral to the domains of Wnt5 staining, confined within the AL boundaries. At 36 hAPF, as high levels of Wnt5 accumulated in the commissure in the drl^{2} mutant (arrowhead in **Figs. 9g and h**), the PN dendrites began to transgress the AL boundaries and project medially towards the region of ectopic Wnt5 enrichment (arrows in **Figs. 9h and h'**). Our results show that in the absence of *drl*, Wnt5 accumulates in the commissure, leading to the formation of ectopic midline glomeruli.

Discussion

The mechanisms by which ingrowing axons sort into precise maps, like those found in the olfactory glomeruli or the somatosensory barrels, are poorly understood. Deafferentation and transplantation experiments revealed that ingrowing axons play powerful roles in specifying the maps within initially homogenous structures[12,13,40]. However, little is known about how the ingrowing axons carry out these feats. In this report we show that ingrowing ORN axons express Wnt5, which contributes to organizing the glomerular pattern of the *Drosophila* olfactory system. We also show that the Drl receptor tyrosine kinase acts in glial cells to modulate Wnt5 signalling. This novel interaction between ORN axons and glia reveals a powerful role for ORN axon-glia interactions in regulating the precise neural circuitry of *Drosophila* AL.

wnt5 is an Anterograde Signal that Organizes the AL

The *wnt5* mutant displays characteristic disruptions of the olfactory map. Many dorsomedial glomeruli are displaced ventrally, resulting in the ALs acquiring a heart shaped appearance, and the large commissure that connects the two ALs in the wild type fails to form. A critical question was whether the glomerular defects arise as a consequence of axons failing to cross the midline. Our unpublished observations that the ALs are apparently patterned normally despite the absence of the commissure in the Neuroglian mutant (Chen et. al., manuscript in preparation) indicates that AL malformation does not necessarily result when ORN axons fail to cross the midline.

In contrast to the loss-of-function defects, overexpression of *wnt5* leads to the displacement of glomeruli into the midline. Examination of the ORN axons in the *wnt5* mutant shows that they take circuitous paths to their targets and frequently misproject to dorsal regions of the brain. Consistent with a role for *wnt5* in AL development, the AL defects appear during the pupal stage, when ORN axon targeting and glomerular development occur. Our genetic mosaic and cell-type specific rescue experiments indicate that *wnt5* is required in the ORNs. Antibody stainings indicate that the Wnt5 protein is enriched on the dendrites of the PNs, where it presumably accumulates subsequent to its secretion by ORNs. In addition to the PN dendrites,

Wnt5 also accumulates in the antennal commissure in the *drl*^{2} mutant. We propose that Wnt5 is a signal by which ingrowing ORN axons direct the development of their target field.

d*rl* Acts in Glial Cells to Regulate Antennal Lobe Development

Mutation in the *drl* gene also produces disruptions of the olfactory map. However, unlike the stereotyped shifts of glomeruli seen in the *wnt5* mutant, the glomeruli are randomly positioned, split or apparently missing at times in the *drl* mutant. The glomeruli also tend to form at the midline. Furthermore, the ORN axons take indirect routes to their targets, as in the *wnt5* mutant. That *drl* functions in development is supported by the observation that AL defects are visible at 40 hAPF, the time when ORN axon targeting and glomerular development take place.

Antibody staining shows that the Drl protein is highly expressed by cells that are intimately associated with the ingrowing ORN axons, the PNs and glia. In the PNs, Drl is enriched in the dendrites of nascent glomeruli. Four of these glomeruli also accumulate the Wnt5 protein in the wild type and *drl* mutant. The Drl protein is also highly expressed in the TIFR, a donut-shaped midsaggittal structure in the brain composed of glial cells[34]. Genetic ablation of the TIFR revealed that it plays a powerful role in the development of neuropil structures adjacent to the midline[41]. Our histological studies show that the TIFR is closely associated with the nascent ALs and that glial processes are closely associated with the commissural bridge that connects the opposite ALs. Interestingly, this glial bridge also expresses the Drl protein. Several observations indicate that *drl* functions in the TIFR to regulate *wnt5* function. First, removal of *drl* from single-PN clones did not disrupt the development and morphology of the PNs. Second, neuronal expression of *drl* in the *drl*^{2} mutant background did not rescue the mutant phenotype. Third, expression of *UAS-drl* under the control of *Repo-Gal4* strongly rescued the *drl* mutant phenotype, suggesting that *drl* functions in glial cells. While we cannot rule out roles for drl in the PNs, collectively, our observations suggest that *drl* functions predominantly in glial cells to regulate AL development. That the midline glia play an important role in AL development is also supported by our unpublished observations that ablation of the TIFR glia results in severe disruption of glomerular structures (Chen et. al., manuscript in preparation).

Drl Regulates AL Development through its extracellular WIF domain

The Drl protein is a member of the RYK receptor tyrosine kinase-related family, which have recently emerged as important receptors for Wnt proteins[42]. Members of this family possess an extracellular WIF domain, and an intracellular “atypical” kinase domain, so called because a number of conserved residues in the domain have been substituted with nonconserved amino acids. The mechanisms by which Drl transduces extracellular Wnt binding into intracellular changes are poorly characterized. Experiments in cultured cells however, indicate the involvement of Disheveled in a pathway that culminates in the activation of TCF/Lef-dependent genes[43]. Our ability to rescue the *drl* mutant phenotype afforded us the opportunity to probe the requirement for the major domains of Drl in glomerular patterning.
Mutation of the conserved K371 residue, which is essential for the kinase activity[38], to an alanine did not significantly impair rescue by the transgene. It was previously reported that, while kinase activity is dispensable for both embryonic neuronal and muscle fiber pathfinding, the intracellular domain is required for proper midline axon pathfinding in the embryonic ventral nerve cord[21]. Results from another study have also suggested that the Drl intracellular domain has a regulatory function[39]. We found that expression of a truncated Drl protein lacking the entire

cytoplasmic domain significantly rescued the AL defects, indicating that the cytoplasmic domain is likely not essential for AL development. In contrast to the apparent lack of a requirement for the cytoplasmic domain, deletion of the extracellular WIF domain completely abolished Drl's ability to rescue the mutant phenotype. These results suggest that Drl functions in AL patterning predominantly through its extracellular WIF domain.

Drl Modulates Wnt5 Function During Antennal Lobe Development

To further understand the relationship between *wnt5*, expressed in the ORNs, and *drl*, expressed in glia, we examined their genetic interactions. The phenotypic similarity between the *drl* loss-of-function and the *wnt5*-overexpressing mutant raises the intriguing possibility that the two genes act antagonistically in AL development. Indeed, expression of a weak *wnt5* transgene in the ORNs, which has no effect in the wild type, triggers the formation of ectopic glomeruli in the drl^{2} mutant. Thus, *wnt5* and *drl* function in opposition to each other in AL development. To ascertain the relative positions of *wnt5* and *drl* in this signalling pathway, we generated animals carrying null mutations in both genes. We found that the $wnt5^{400}$*;* drl^{2} double mutant displays a distinct *wnt5* phenotype. The *wnt5* mutation is therefore epistatic to the *drl* mutation, indicating that *wnt5* likely functions downstream of *drl* in AL development. This conclusion is also supported by the observations that, whereas the removal of a copy of *wnt5* gene strongly suppresses the *drl* homozygous mutant phenotype, the removal of a copy of *drl* gene has no effect on the *wnt5* homozygous mutant phenotype. The genetic data that *drl* downregulates *wnt5* function is further supported by our observation that Wnt5 protein significantly accumulates in the commissure in the absence of Drl. Taken together, our genetic and histological data indicate that *drl* acts to inhibit the activity of *wnt5* during glomerular development.

How might Drl inhibit the function of Wnt5? One possibility is that Drl inhibits Wnt5 function simply by sequestering and/or endocytosing Wnt5, thus limiting its interaction with another as yet unidentified receptor. This receptor might be one of the other Drosophila Ryks, or members of the Frizzled family, one of which, *fz2*, has been shown to interact genetically with *wnt5* to stabilize axons of the Drosophila visual system[23]. This hypothesis is supported by our observations that Drl function in the ALs only apparently requires its extracellular Wnt5-binding WIF domain but not its cytoplasmic domain. Alternatively, Drl may directly interact with another receptor and Wnt5, as observed previously for its mammalian ortholog, Ryk, and members of the Wnt5 and Frizzled families[43]. This interaction could inhibit or alter the signal transduced from the membrane. We did not observe, however, a requirement for Drl's cytoplasmic domain, which presumably would be needed for interaction with downstream components of a signalling pathway, suggesting that transduction of the Wnt5 signal by Drl alone is unlikely to play a major role in patterning the ALs.

Afferent-Glia Interaction Specifies the Glomerular Map

How do glial cells interact with the ORN axons to specify the olfactory map? In the development of the olfactory glomeruli in *Manduca*, glial cells migrate to surround the protoglomeruli in response to the ingrowing ORN axons[44]. It was proposed that the glia form scaffolds, within which neuronal processes arborize. However, glial processes in *Drosophila* were reported to invade the AL neuropil only after the glomeruli are formed[30], suggesting that such a mechanism is unlikely to operate in *Drosophila*. Our data suggest that the ingrowing ORN axons contribute to AL patterning through secretion of Wnt5 and glial cells locally regulate Wnt5 actions through Drl.

We propose the following working model for how Wnt5-Drl signalling might regulate glomerular patterning. Ingrowing ORN axons express Wnt5, which is important for the precise organization of the glomeruli and pathfinding of the ORN axons, such as those crossing the midline, or projecting to the dorsomedial region of the ALs. Normal AL development requires that the Wnt5 signal be locally attenuated by the TIFR glial cell-expressed Drl protein. In the *wnt5* mutant, the lack of Wnt5 signalling results in the failure of ORN axons to cross the midline and the establishment of glomeruli in more ventral positions. In the *drl* mutant, Wnt5 accumulates at the midline and presumably inappropriately signals through another receptor, resulting aberrant ORN axon targeting to the midline, and the formation of ectopic glomeruli at the dorsomedial corner of the AL and at the midline. This phenotype is remarkably similar to that seen when Wnt5 is forcibly expressed in the ORNs. Further studies will hopefully help to unravel the precise mechanisms by which Wnt5 and Drl act together to specify the patterning of the *Drosophila* olfactory map.

Acknowledgments

We thank the Bloomington Stock Center for the fly lines; A. Hofbauer for generous gift of the nc82 antibody; and W. Zhou for construction of the UAS-drl transgenic fly line. This work is supported by grants from NIH/NIDCD (DC5408-01) and the Roy J. Carver Charitable Trust (#03-27) (H.H.), as well as ASPASIA and Pionier (J.N.) and a Genomics grant (L.F. and J.N.) from the "Nederlandse Organisatie voor Wetenschappelijk Onderzoek".

Author Contributions

Y.W., Y.Y., C.Y., and R.O. conducted the experiments in the laboratory of H.H.; and R.R.W. conducted the experiments in the laboratory of J.N.N. and L.G.F. Y.W., Y.Y. and H.H. analyzed the data; and H.H. wrote the manuscript with contribution from all other authors.

References

1 Mombaerts, P. Axonal wiring in the mouse olfactory system. *Annu Rev Cell Dev Biol* **22**, 713-737 (2006).
2 Dynes, J. L., and Ngai, J. Pathfinding of olfactory neuron axons to stereotyped glomerular targets revealed by dynamic imaging in living zebrafish embryos. *Neuron* **20**, 1081-1091. (1998).
3 Potter, S. M.*, et al.* Structure and emergence of specific olfactory glomeruli in the mouse. *J Neurosci* **21**, 9713-9723 (2001).
4 Lin, D. M., and Ngai, J. Development of the vertebrate main olfactory system. *Curr Opin Neurobiol* **9**, 74-78. (1999).
5 Key, B., and St John, J. Axon Navigation in the Mammalian Primary Olfactory Pathway: Where to Next? *Chem Senses* **27**, 245-260 (2002).
6 Ang, L. H., Kim, J., Stepensky, V., and Hing, H. Dock and Pak regulate olfactory axon pathfinding in Drosophila. *Development* **130**, 1307-1316 (2003).
7 Hummel, T.*, et al.* Axonal targeting of olfactory receptor neurons in Drosophila is controlled by Dscam. *Neuron* **37**, 221-231 (2003).
8 Hummel, T., and Zipursky, S. L. Afferent induction of olfactory glomeruli requires N-cadherin. *Neuron* **42**, 77-88 (2004).
9 Miyasaka, N.*, et al.* Robo2 is required for establishment of a precise glomerular map in the zebrafish olfactory system. *Development* **132**, 1283-1293 (2005).
10 Stout, R. P., and Graziadei, P. P. Influence of the olfactory placode on the development

of the brain in Xenopus laevis (Daudin). I. Axonal growth and connections of the transplanted olfactory placode. *Neuroscience* **5**, 2175-2186 (1980).

11 Oland, L. A., Orr, G., and Tolbert, L. P. Construction of a protoglomerular template by olfactory axons initiates the formation of olfactory glomeruli in the insect brain. *J Neurosci* **10**, 2096-2112. (1990).

12 Graziadei, P. P., and Kaplan, M. S. Regrowth of olfactory sensory axons into transplanted neural tissue. 1. Development of connections with the occipital cortex. *Brain Res* **201**, 39-44. (1980).

13 Schneiderman, A. M., Matsumoto, S. G., and Hildebrand, J. G. Trans-sexually grafted antennae influence development of sexually dimorphic neurones in moth brain. *Nature* **298**, 844-846 (1982).

14 Ang, L. H.*, et al.* Lim kinase regulates the development of olfactory and neuromuscular synapses. *Dev Biol* **293**, 178-190 (2006).

15 Oland, L. A., and Tolbert, L. P. Multiple factors shape development of olfactory glomeruli: insights from an insect model system. *J Neurobiol* **30**, 92-109. (1996).

16 Stocker, R. F., Lienhard, M. C., Borst, A., and Fischbach, K. F. Neuronal architecture of the antennal lobe in Drosophila melanogaster. *Cell Tissue Res* **262**, 9-34. (1990).

17 Gao, Q., Yuan, B., and Chess, A. Convergent projections of Drosophila olfactory neurons to specific glomeruli in the antennal lobe. *Nat Neurosci* **3**, 780-785. (2000).

18 Vosshall, L. B., Wong, A. M., and Axel, R. An olfactory sensory map in the fly brain. *Cell* **102**, 147-159 (2000).

19 Cadigan, K. M., and Nusse, R. Wnt signalling: a common theme in animal development. *Genes Dev* **11**, 3286-3305 (1997).

20 Moon, R. T., Bowerman, B., Boutros, M., and Perrimon, N. The promise and perils of Wnt signalling through beta-catenin. *Science* **296**, 1644-1646 (2002).

21 Yoshikawa, S., McKinnon, R. D., Kokel, M., and Thomas, J. B. Wnt-mediated axon guidance via the Drosophila Derailed receptor. *Nature* **422**, 583-588 (2003).

22 Fradkin, L. G.*, et al.* The Drosophila Wnt5 protein mediates selective axon fasciculation in the embryonic central nervous system. *Dev Biol* **272**, 362-375 (2004).

23 Srahna, M.*, et al.* A Signalling Network for Patterning of Neuronal Connectivity in the Drosophila Brain. *PLoS Biol* **4** (2006).

24 Zhang, D.*, et al.* Misexpression screen for genes altering the olfactory map in Drosophila. *Genesis* **44**, 189-201 (2006).

25 Jhaveri, D., Sen, A., and Rodrigues, V. Mechanisms underlying olfactory neuronal connectivity in Drosophila-the atonal lineage organizes the periphery while sensory neurons and glia pattern the olfactory lobe. *Dev Biol* **226**, 73-87. (2000).

26 Hofbauer, A. (1991) Eine Bibliothek monoklonaler Antikorper gegen das Gehirn von Drosophila melanogaster., Habilitation Thesis, University of Wurzburg, Wurzburg.

27 Wagh, D. A.*, et al.* Bruchpilot, a protein with homology to ELKS/CAST, is required for structural integrity and function of synaptic active zones in Drosophila. *Neuron* **49**, 833-844 (2006).

28 Couto, A., Alenius, M., and Dickson, B. J. Molecular, anatomical, and functional organization of the Drosophila olfactory system. *Curr Biol* **15**, 1535-1547 (2005).

29 Fishilevich, E., and Vosshall, L. B. Genetic and functional subdivision of the Drosophila antennal lobe. *Curr Biol* **15**, 1548-1553 (2005).

30 Jefferis, G. S.*, et al.* Developmental origin of wiring specificity in the olfactory system of Drosophila. *Development* **131**, 117-130 (2004).

31 Sweeney, L. B.*, et al.* Temporal target restriction of olfactory receptor neurons by Semaphorin-1a/PlexinA-mediated axon-axon interactions. *Neuron* **53**, 185-200 (2007).

32. Lee, T., and Luo, L. Mosaic analysis with a repressible neurotechnique cell marker for studies of gene function in neuronal morphogenesis. *Neuron* **22**, 451

461. (1999).
32 Dura, J. M., Taillebourg, E., and Preat, T. The Drosophila learning and memory gene linotte encodes a putative receptor tyrosine kinase homologous to the human RYK gene product. *FEBS Lett* **370**, 250-254 (1995).
33 Simon, A. F., Boquet, I., Synguelakis, M., and Preat, T. The Drosophila putative kinase linotte (derailed) prevents central brain axons from converging on a newly described interhemispheric ring. *Mech Dev* **76**, 45-55 (1998).
34 Stocker, R. F., Heimbeck, G., Gendre, N., and de Belle, J. S. Neuroblast ablation in Drosophila P[GAL4] lines reveals origins of olfactory interneurons. *J Neurobiol* **32**, 443-456. (1997).
35 Jefferis, G. S., Marin, E. C., Stocker, R. F., and Luo, L. Target neuron prespecification in the olfactory map of Drosophila. *Nature* **414**, 204-208. (2001).
36 Sen, A., Shetty, C., Jhaveri, D., and Rodrigues, V. Distinct types of glial cells populate the Drosophila antenna. *BMC Dev Biol* **5**, 25 (2005).
37 Hanks, S. K., Quinn, A. M., and Hunter, T. The protein kinase family: conserved features and deduced phylogeny of the catalytic domains. *Science* **241**, 42-52. (1988).
38 Taillebourg, E., Moreau-Fauvarque, C., Delaval, K., and Dura, J. M. In vivo evidence for a regulatory role of the kinase activity of the linotte/derailed receptor tyrosine kinase, a Drosophila Ryk ortholog. *Dev Genes Evol* **215**, 158-163 (2005).
39 Schlaggar, B. L., and O'Leary, D. D. Potential of visual cortex to develop an array of functional units unique to somatosensory cortex. *Science* **252**, 1556-1560 (1991).
40 Hitier, R., Simon, A. F., Savarit, F., and Preat, T. no-bridge and linotte act jointly at the interhemispheric junction to build up the adult central brain of Drosophila melanogaster. *Mech Dev* **99**, 93-100 (2000).
41 Bovolenta, P., Rodriguez, J., and Esteve, P. Frizzled/RYK mediated signalling in axon guidance. *Development* **133**, 4399-4408 (2006).
42 Lu, W., Yamamoto, V., Ortega, B., and Baltimore, D. Mammalian Ryk is a Wnt coreceptor required for stimulation of neurite outgrowth. *Cell* **119**, 97-108 (2004).
43 Oland, L. A., Tolbert, L. P., and Mossman, K. L. Radiation-induced reduction of the glial population during development disrupts the formation of olfactory glomeruli in an insect. *J Neurosci* **8**, 353-367. (1988).
44 Toba, G*., et al.* The gene search system. A method for efficient detection and rapid molecular identification of genes in Drosophila melanogaster. *Genetics* **151**, 725-737 (1999).

Supplementary Data

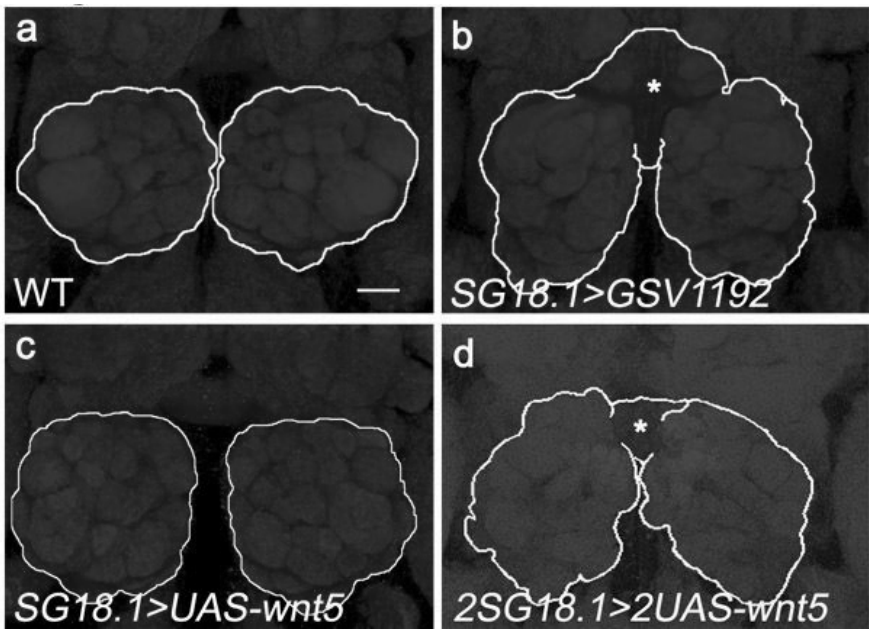

Supplementary Fig. 1. Function of Wnt5 in the AL is dosage-dependent ALs of animals expressing various levels of *wnt5* were stained with the nc82 antibody (red) to visualize the shape of the ALs and the pattern of the glomeruli. (**a**) In the wild type, the ALs are spherical and the glomeruli are found within the confines of the ALs (outlined). (**b**) In animals expressing *P{GS1}1192* under the control of *SG18.1-Gal4*, the stereotyped pattern of glomeruli is disrupted and ectopic glomeruli appear at the midline (asterisk) in 100% of the ALs. (**c**) In animals bearing one copy of *UAS-wnt5* and one copy *SG18.1-Gal4*, the structure of the ALs and the arrangement of the glomeruli appear wild type. (**d**) In animals bearing two copies of *UAS-wnt5* and two copies *SG18.1-Gal4*, the glomerular pattern is disrupted and ectopic glomeruli appear at the midline (asterisk). This phenotype mimics the phenotype of the *P{GS1}1192*-expressing animals. Scale bar is 20 μm. (see Appendix: Selected Color Figures)

Figure S2

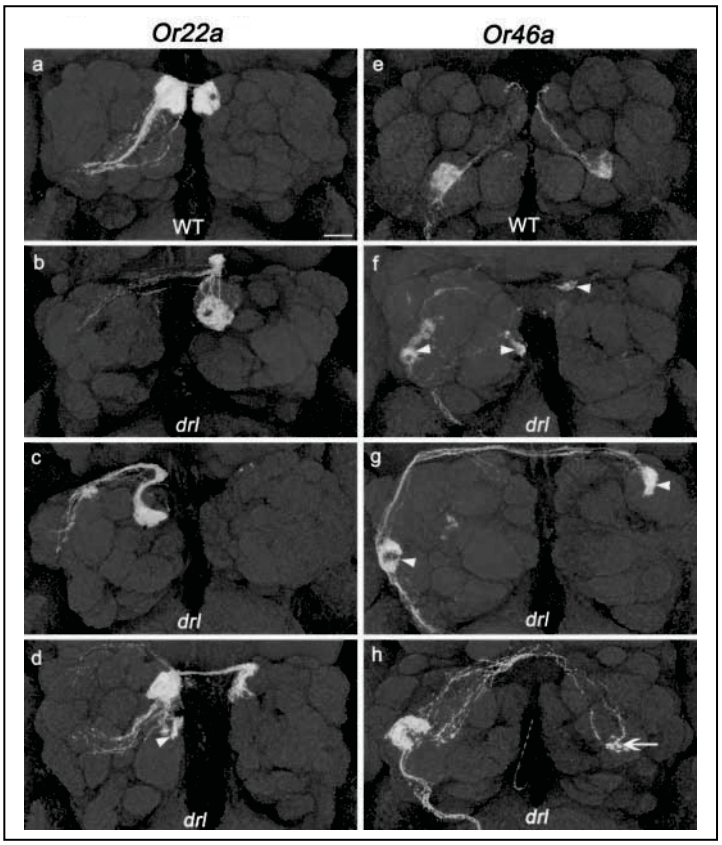

Figure S3

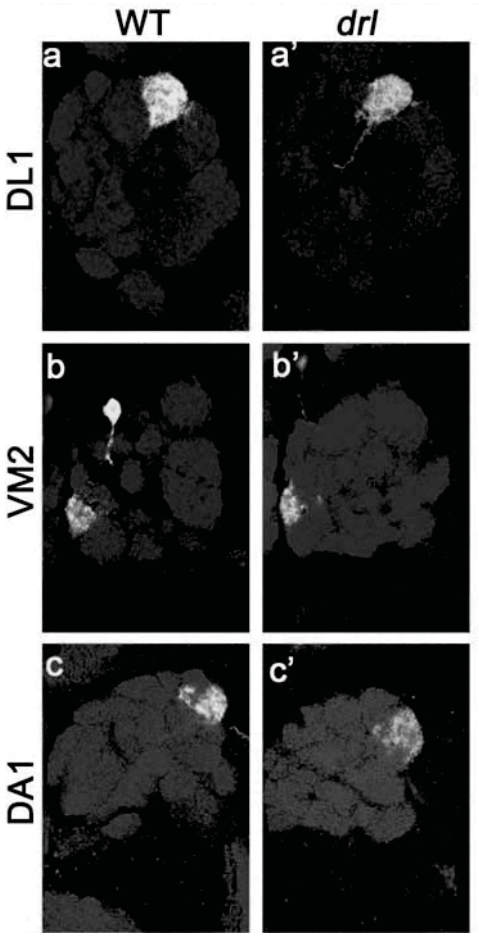

Figure S2. *drl* mutant defects occur both contralaterally and ipsilaterally
The axons of *Or*22a and *Or46a* were examined 10 days after excising the left antenna (**a-d**), or maxillary palp (**e-h**) (causing ORNs axons to degenerate). (**a**) In wild-type animals, *Or22a* axons project through a stereotyped pathway to terminate at an invariant position in the ipsilateral and contralateral ALs. In *drl* mutant animals, *Or22a* axons exhibit a number of defects. (**b**) Some axons fail to form glomeruli in the ipsilateral AL. (**c**) Some axons fail to cross the midline and form glomeruli in the contralateral AL. (**d**) In addition, some axons form ectopic glomeruli in the ipsilateral AL (arrowhead). (**e**) In wild-type animals, *Or46a* axons project through a stereotyped pathway to terminate at an invariant position in the ipsilateral and contralateral ALs. (**f, g**) In *dr*l mutant animals, *Or46a* axons often mistarget in both ipsilateral and contralateral ALs (arrowheads). (**h**) Some *Or46a* axons inefficiently project to the contralateral side resulting in a smaller glomerular size on that side (arrow). Scale bar is 20 μm. (see Appendix: Selected Color Figures)

Figure S3. Dendritic pattern of drl mutant clones is normal
Preparations of wild-type (**a, b, c**) and drl^2 mutant (**a', b', c**') PN clones generated using the MARCM technique are shown. (**a**) A wild-type dorsal PN showing dendritic innervation of the DL1 glomerulus. (**a'**) A drl^2 mutant dorsal PN showing normal dendritic targeting of the DL1 glomerulus. (**b**) A wild-type dorsal PN innervating the VM2 glomerulus. (**b'**) A drl^2 mutant dorsal PN targeting the VM2 glomerulus normally. (**c**) A wild-type lateral PN innervating the DA1 glomerulus. (**c'**) A drl^2 mutant lateral PN innervating the DA1 glomerulus normally. (see Appendix: Selected Color Figures)